3

Molecular Spectroscopy

3.1 Introduction

Interstellar molecules – to be precise, diatomic radicals – were first discovered through their electronic transitions in the visual and near-UV regions of the spectrum in the 1930s. The diffuse interstellar bands (DIBs) – a set of some 400 interstellar absorption lines in the visible and far-red parts of the stellar spectra – date back even further. The DIBs also find their origin in molecular electronic transitions. In the solar system, the spectra of comets are dominated by emission bands due to simple molecular radicals and cations. Typically, molecular bond strengths are some 5–10 eV and electronic transitions occur in the far-UV. If there are low lying empty orbitals – as for radicals or ions – transitions shift toward longer wavelengths.

Vibrational transitions involve motions of the atoms in the molecule. They shift therefore by a factor $\sqrt{m_e/M}$ toward lower frequencies. As this is the mid-IR range of the spectrum, first observations of interstellar molecules in the infrared had to await the development of sensitive detectors and the opening up of this window in 1970s. Ro-vibrational transitions of molecules are routinely seen in absorption in the spectra of a wide variety of objects including cool giants (later than spectral type K), brown dwarfs, (exo)planet atmospheres, Hot cores associated with high mass protostars, and obscured galactic nuclei such as UltraLuminous Infrared Galaxies. In emission, the ro-vibrational transitions of H_2 pumped by UV photons are prominent in the spectra of photodissociation regions. These spectra also show strong emission bands due to vibrational fluorescence of UV-pumped polycyclic aromatic hydrocarbon molecules. The mid infrared spectra of all star-forming galaxies are dominated by these bands. Molecular vibrational emission bands are also present in the spectra of comets, protoplanetary disks, and shocks in molecular clouds. Vibrational transitions correspond to energies of typically a few hundred to a thousand degrees.

The discovery of (pure) rotational transitions due to interstellar molecules dates back to the late 1960s. As detectors improved, telescopes grew in size, and the sub-millimeter sky opened up, the list of molecules detected through their pure rotational transitions steadily grew over the years. When ALMA entered its operational phase, the pace of new molecular identifications increased manyfold. The energies associated with molecular rotations are typically a few degrees, depending on the moment of inertia, and occur in the

https://doi.org/10.1017/9781316718490.004 Published online by Cambridge University Press

(sub)-millimeter to far-infrared. Rotational transitions dominate the cooling of molecular clouds and in particular regions of star formation. The multitude of lines also provide powerful probes of the physical conditions in the emitting gases.

This Chapter introduces various aspects of molecular spectroscopy including energy levels, transition frequencies, selection rules, and transition strengths. There are separate sections on pure rotational transitions, on vibrational and ro-vibrational transitions, and on electronic spectra. Rotational spectroscopy has developed into a main staple of astronomy and a course would do well by discussing in depth the rotational spectra of linear molecules (Section 3.2.2). Symmetric top molecules (Section 3.2.3) present "merely" variations on a theme, while the spectra of asymmetric top molecules (Section 3.2.4) are too complex to be caught in simple rules (but are of great individual interest). These sections can be left for background reading. That also holds for the sections on hyperfine splitting, Λ-doubling, nuclear spin, and partition function (Section 3.2.5–3.2.8). The section on transitions strength (Section 3.2.9) is important for all students, though. In the vibrational spectroscopy section, Hooke's law and molecular identifications are important for all astronomy students while partition function and gas phase ro-vibrational spectra might be assigned to background reading. Electronic spectroscopy can also be left to the individual students interested in this aspect. The chapter ends with a discussion of the spectroscopy of three specific molecules, H_2, CO, and H_2CO (Section 3.5), and together they serve well as a framework to introduce students to relevant concepts introduced in this chapter. Finally, issues involving molecular excitation, emission intensities, and analysis of molecular observations are presented in Chapter 4.

3.2 Rotational Spectroscopy

3.2.1 Energy Levels

Rotational transitions arise from the rotation of the permanent dipole interacting with an oscillating electromagnetic field. Typically, this occurs in the microwave region of the spectrum. Rotational transitions are – to first order – set by the moments of inertia of the molecule. Working in the center of mass frame, we can define three orthogonal axes at the center of mass of the molecule, a, b, and c. The moments of inertia are then,

$$I_j = \sum_i m_i r_i^2 \quad j = a, b, c \tag{3.1}$$

where m_i is the mass of atom i at distance r_i from the center of mass and the summation is over all atoms. By convention $I_c \geq I_b \geq I_a$. As an example, for a diatomic molecule, the moment of inertia is $I = \mu R^2$ with μ the reduced mass and R the distance between the atoms. For a rigid rotor,[1] the rotational structure is set by the symmetry of the molecule.

[1] No distortion under rotation.

https://doi.org/10.1017/9781316718490.004 Published online by Cambridge University Press

Table 3.1 *Classification of rotors*

Moment of inertia	Symmetry	Rotational constants	Example
$I_a = I_b = I_c$	Spherical top	$A = B = C$	CH_4[a], SF_6[a]
$I_a = 0, I_b = I_c$	Linear molecule	$A = \infty, B = C$	CO, CO_2[a]
$I_a < I_b = I_c$	Prolate symmetric top	$A > B = C$	C_2H_6
$I_a = I_b < I_c$	Oblate symmetric top	$A = B > C$	C_6H_6
$I_a < I_b < I_c$	Asymmetric top	$A > B > C$	H_2O

[a]These symetric molecules have no permanent dipole and therefore no pure rotational spectrum.

Table 3.1 summarizes the classification. For a rigidly rotating molecule, the rotational energy levels can be described classically by the rotations of a rigid body,

$$E_r = \frac{1}{2}\left(I_a\omega_a^2 + I_b\omega_b^2 + I_c\omega_c^2\right) = \frac{1}{2}\left(\frac{\mathcal{J}_a^2}{I_a} + \frac{\mathcal{J}_b^2}{I_b} + \frac{\mathcal{J}_c^2}{I_c}\right), \tag{3.2}$$

with ω_j the rotational frequency and $\mathcal{J}_j$ the angular momentum ($= I_j\omega_i$).

3.2.2 Linear Molecules

We will start with a simple system, a linear molecule. The quantum mechanical analog is then, $\mathcal{J} = \sqrt{J\,(J+1)}\hbar$ with J ($= 0, 1, 2, \ldots$), the rotational quantum number, and we have,

$$E_r = \frac{J\,(J+1)\,\hbar^2}{2I}. \tag{3.3}$$

We can write this in terms of the rotational constant, B_e,

$$B_e = \frac{h}{8\pi^2 cI} \tag{3.4}$$

in wavenumbers, as,

$$\frac{E_r}{hc} = B_e\,J\,(J+1)\,. \tag{3.5}$$

As a guide,

$$B_e \simeq \frac{17}{I\ (\text{amu Å}^2)}\ \text{cm}^{-1} \simeq \frac{500}{I\ (\text{amu Å}^2)}\ \text{GHz}. \tag{3.6}$$

Radiative rotational transitions are allowed for $\Delta J = \pm 1$, and the spectrum consists of a set of evenly spaced lines in frequency space (Figure 3.1); viz.,

$$\nu\,(J+1 \rightarrow J) = \frac{E\,(J+1) - E\,(J)}{hc} = 2B\ (J+1)\,. \tag{3.7}$$

https://doi.org/10.1017/9781316718490.004 Published online by Cambridge University Press

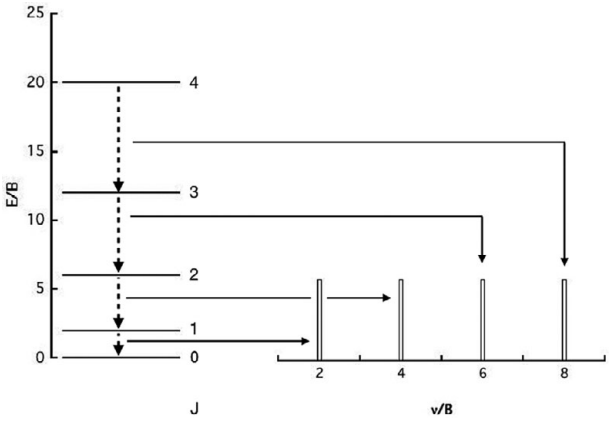

Figure 3.1 Left: Schematic rotational energy level diagram for a linear molecule. Energy – in units of the rotational constant, B – increases upward. The individual levels have been labeled with their J-value. Allowed transitions correspond to $\Delta J = \pm 1$. Right: To first order, the spectrum of a linear molecule consists of a set of equidistant lines. Frequency is in units of the rotational constant.

As B_e decreases with $1/I$, molecules consisting of heavier atoms will have transitions at lower frequencies. So, the lowest frequencies for CS and CO are at aproximately 49 and 115 GHz, respectively (cf. Table 3.3). Transitions of light hydrides occur in the far-infrared (e.g. HF at 1.2 THz), while the groundstate pure rotational transition of H_2 falls at 10.6 THz (28 μm).

A rotating molecule will pull apart and the moment of inertia will increase with increasing rotation. Allowing for this centrifugal stretching, the energy levels become

$$\frac{E_r}{hc} = B_e\, J\,(J+1) - D_e\, J^2\,(J+1)^2\,, \tag{3.8}$$

with D_e the centrifugal distortion constant. The line frequencies are then,

$$\nu\,(J+1 \rightarrow J) = 2B\;(J+1) - 4D_e\,(J+1)^3 \tag{3.9}$$

$$= 2B\;(J+1)\left(1 - \frac{2D_e}{B}\,(J+1)^2\right). \tag{3.10}$$

Centrifugal distortion will thus destroy the constant separation of rotational transitions in the spectrum of a rigid rotor. The way it is written above, centrifugal distortion represents a correction factor on B and this correction depends on the magnitude of the angular momentum. Obviously, for faster spinning molecules, the bond will lengthen more and the increased moment of inertia results in a decreased rotational constant. For a harmonic oscillator, $D_e = 4B_e^3/\nu_e^2$ with ν_e the vibrational frequency (in cm^{-1}). Centrifugal distortion is, thus, a "small" correction factor to the frequency of the rotation; i.e. $D_e/B_e = 4\,(B_e/\nu_e)^2 \ll 1$. Consider CO with $\nu_e = 2170\ \mathrm{cm}^{-1}$ and $B_e = 1.93\ \mathrm{cm}^{-1}$; the correction

https://doi.org/10.1017/9781316718490.004 Published online by Cambridge University Press

factor is 8.5×10^{-7}. In astronomy, for pure rotational transitions, this clearly has to be taken into account ($\Delta v \simeq 0.26\,(J+1)^2$ km/s). And even for ro-vibrational transitions (see Section 3.3.4), this correction factor amounts to 0.1 cm^{-1} on a level separation of 1 cm^{-1} at $J = 10$.

Anharmonic effects can be included as higher order correction terms. Vibrational motions occur at much higher frequency than rotations and hence a molecule will vibrate many, many times during one rotation. As rotations depend on the average of $1/R^2$, even for harmonic oscillators, the rotational constant will vary with vibrational excitation. For anharmonic oscillators, the rotational constant will decrease with increasing vibrational excitation as the average separation between the atoms increases. The dependence of the spectrum on the vibrational state is captured in small correction factors on the rotational constant as well as on the centrifugal distortion constant that depend on the vibrational quantum number of the modes involved,

$$B_v = B_e - \alpha_e \left(v + \frac{1}{2}\right) + \cdots \tag{3.11}$$

$$D_v = D_e + \beta_e \left(v + \frac{1}{2}\right) + \cdots . \tag{3.12}$$

These are small correction factors. If we include the cubic term in the potential expansion, we have

$$\alpha_e = \frac{24 B_e^3 R_e^3 g}{\omega_e^3} - \frac{6 B_e^2}{\omega_e}, \tag{3.13}$$

where g is the coefficient of the cubic term in the expansion (in units of cm^{-1}) and the fundamental vibrational frequency, ν_e, and the anharmonicity parameter, $x_e\nu_e$, are described in Section 3.3.1. Often this parameter is expressed using a Morse potential,

$$\alpha_e = -6 \left(\frac{B_e}{\nu_e}\right) \left(B_e - \sqrt{x_e \nu_e B_e}\right). \tag{3.14}$$

As the Morse potential is fully described by the bond energy, ν_e and $x_e\nu_e$, no new parameter is introduced and differences of this expression with measurements are then an indication of the deviation of the actual potential from the Morse potential. Expanding the potential again to cubic terms, we have for β_e,

$$\beta_e = D_e \left(\frac{8\omega_e x_e}{\omega_e} - \frac{5\alpha_e}{B_e} - \frac{\alpha_e^2 \omega_e}{24 B_e^3}\right). \tag{3.15}$$

However, β_e is a small correction on a small correction and is often neglected.

https://doi.org/10.1017/9781316718490.004 Published online by Cambridge University Press

3.2.3 Symmetric Top Molecules

Let's now consider a symmetric top molecule (Table 3.1). Two moments of inertia are the same – say, $I_b = I_c$ (a prolate symmetric top) – so we can write,

$$E_r = \frac{\mathcal{J}_a^2}{2I_a} + \frac{\mathcal{J}_b^2 + J_c^2}{2I_b}, \tag{3.16}$$

with $\mathcal{J}^2 = \mathcal{J}_a^2 + \mathcal{J}_b^2 + \mathcal{J}_c^2$, we then have,

$$E_r = \frac{\mathcal{J}^2}{2I_b} + \mathcal{J}_a^2 \left(\frac{1}{2I_a} - \frac{1}{2I_b}\right). \tag{3.17}$$

We again make the classical to quantum mechanics transformation, $\mathcal{J}^2 \rightarrow J^2 (J+1)\hbar^2$. As there are two main directions of rotation, there are two quantum numbers. Introducing K as the projection on the molecular axis – e.g. a for prolate molecules (and c for oblate species; Table 3.1) – we have $\mathcal{J}_a = K\hbar$. As J_a is quantized, the total angular momentum J can only take a few specific directions. With this, we arrive at,

$$\frac{E_r}{hc} = BJ(J+1) + (A-B)K^2, \tag{3.18}$$

where A and B are the rotational constants, $A = h/8\pi^2 c I_a$ and $B = h/8\pi^2 c I_b$. Again, the units for these rotational constants are wavenumbers. For an oblate symmetric top, we have to replace A by C ($= h/8\pi^2 c I_c$). The rotational quantum number, J, is $J = 0, 1, 2, \ldots$. As K is the projection of J, it can attain the values, $K = 0, \pm 1, \pm 2, \ldots, \pm J$. Note that the energy is independent of the sign of K and each J-level has a $2J+1$ fold degeneracy.

As for linear molecules, a correction term for centrifugal distortion can be included,

$$\frac{E_r}{hc} = BJ(J+1) + (A-B)K^2 - D_J J^2 (J+1)^2 - D_{JK} J(J+1) K^2 - D_K K^4, \tag{3.19}$$

(cf. Eq. (3.8)).

The selection rules are $\Delta J = 1$ and, as there is no dipole moment along the symmetry axis (a), the angular momentum along the symmetry axis cannot change due to radiation, and we have $\Delta K = 0$. The rotational frequencies are,

$$\nu_{JK} = 2B(J+1) - 4D_J (J+1)^3 - 2D_{JK} (J+1) K^2. \tag{3.20}$$

If we write this as,

$$\nu_{JK} = \left(2B - 4D_J (J+1)^2 - 2D_{JK} K^2\right)(J+1) \tag{3.21}$$

then we recognize again that the centrifugal distortion is a correction factor to B that depends on K. This represents a small change in the moment of inertia, I_B.

Figure 3.2 illustrates the energy level diagrams for prolate and oblate symmetric tops. We can consider two extremes: $K = J$ with rotation around the molecular axis and $E_{J,K=J}/hc \simeq AJ^2$ and $K = 0$ with rotation perpendicular to the molecular axis and

https://doi.org/10.1017/9781316718490.004 Published online by Cambridge University Press

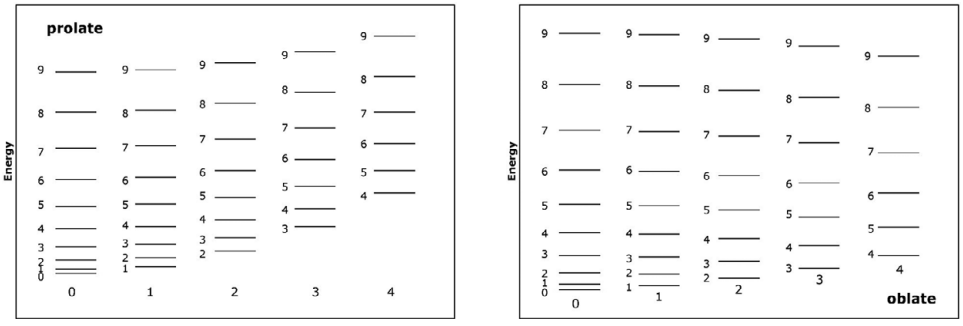

Figure 3.2 Schematic rotational energy level diagram for a prolate (left) and oblate (right) symmetric top molecule. Energy increases upward. The individual levels have been labeled with their J-value. The K-ladders have been shifted horizontally. Allowed transitions occur within each K-ladder. Because K is the projection of J on the molecular symmetry axis, we have $K \leq J$.

$E_{J,K=0}/hc = BJ(J+1)$. In general, for a given K, we recognize the energy level distribution for a linear rotor except that they start with $J = K$ rather than $J = 0$. Note, again, that the energy does not depend on the sign of K and hence, except for $K = 0$, each level is degenerate. Given the selection rule, $\Delta K = 0$, the spectrum is that of a linear rotor. Ignoring the centrifugal distortion, the different K-ladders would coincide but, in reality, transitions will split up. Also, an excited molecule will relax radiatively along its K-ladder and excitation will tend to bottle up in the meta-stable $J = K$ level.

3.2.4 Asymmetric Top Molecules

For asymmetric top molecules, all three moments of inertia are different and there is no simple general formula describing the energy levels. Specifically, $\mathcal{J}$ and its projection on a fixed space axis are constants of motion and J as well as M are good quantum numbers. However, the projection of $\mathcal{J}$ on any of the molecular axes is not conserved and hence none of the molecular axes carries out a simple rotation around $\mathcal{J}$. As a result K is no longer a good quantum number and there is no set of quantum numbers with a simple physical meaning that can be used to describe states. The energy of level, $J_{K_a K_b}$, is generally written as,

$$\frac{E_r}{hc} = \left(\frac{A+C}{2}\right) J(J+1) + \left(\frac{A-C}{2}\right) f(\kappa, K_a, K_b), \tag{3.22}$$

where the asymmetry parameter, κ is given by

$$\kappa = \frac{2B - A - C}{A - C}. \tag{3.23}$$

For a prolate top $\kappa = -1$ while for an oblate top $\kappa = 1$. Extensive tabulations for the function f exist. The spectrum of an asymmetric rotor is thus extremely complex. In

https://doi.org/10.1017/9781316718490.004 Published online by Cambridge University Press

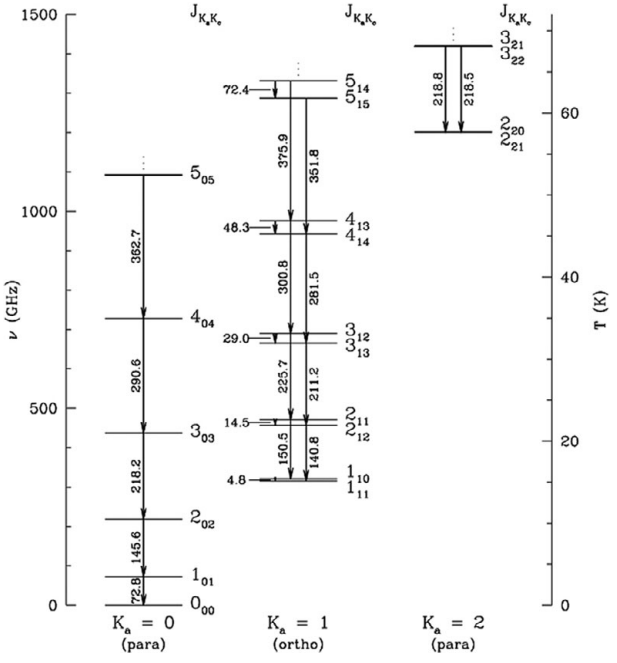

Figure 3.3 Energy level diagram for H_2CO, a near-prolate molecule. Note that formaldehyde has para (K_aK_b are ee or eo) and ortho (K_aK_b are oe or oo, where e=even and o=odd) levels. Figure reproduced with permission from [6]

addition to the irregular distribution of energy levels, the selection rules and transition probabilities between these levels are complicated as the dipole moment may lie in any arbitrary direction with respect to the principal axes of inertia.

When $I_b \simeq I_c \neq I_a$ (prolate), the levels can be represented by $J_{K_aK_b}$, where K_a and K_b are approximate quantum numbers. An analogous approach can be followed for an oblate-like case ($I_b \simeq I_a \neq I_c$). As an example, formaldehyde is a near-prolate molecule ($\kappa = -0.96$). The energy levels show the characteristic pattern of the prolate case (Figure 3.3). The slight deviation from the pure prolate symmetric top case lifts the degeneracy of the levels with $K > 0$ and each level is now split into two. Nevertheless, for the lowest levels, transitions between the different K-ladders are still not allowed. Formaldehyde has para and ortho states, characterized by antiparallel and parallel nuclear spins of the H atoms. These nuclear spin states combine with the rotational states (Section 3.2.7) and para states have K=even while ortho states have K=odd.

H_2O is another example of an asymmetric top molecule ($\kappa = -0.44$). The energy levels are labeled by $J_{K_aK_c}$, where the total angular momentum, J, is a good quantum number while the indices, K_a and K_c, refer to the corresponding prolate and oblate symmetric tops. Sometimes, the pseudo quantum number $\tau = K_a - K_b$ is introduced for labeling convenience. The index τ runs from $J, \ldots, 0, \cdots - J$ (c.f. K for a symmetric top) and

https://doi.org/10.1017/9781316718490.004 Published online by Cambridge University Press

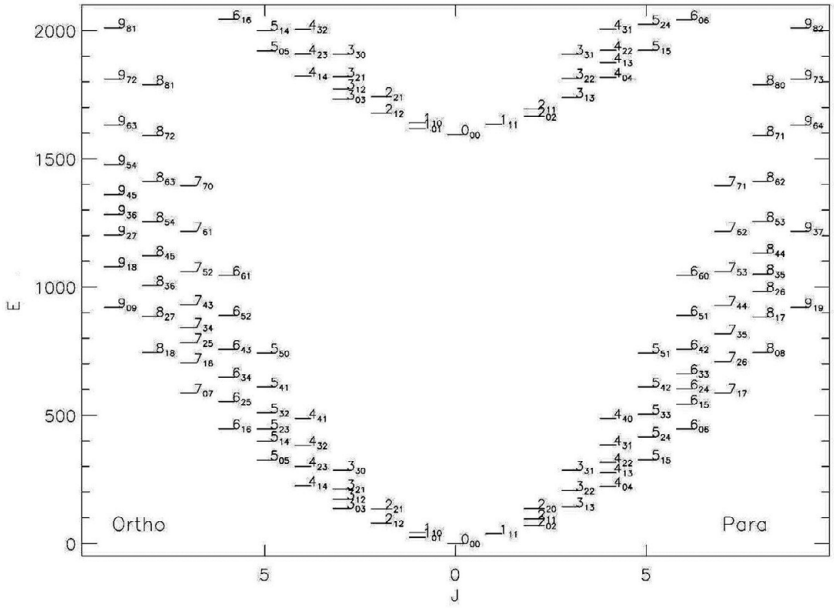

Figure 3.4 Energy level diagram for H_2O. Energies in cm^{-1}. Figure courtesy of F. Helmich

labels the levels in order of decreasing energy. The H_2O energy levels (Figure 3.4) can still be described by $J_{K_aK_c}$. From the symmetry, we have for the selection rules $\Delta J = 0, \pm 1$, $\Delta K_a = \pm 1, \pm 3 \ldots$ and $\Delta K_b = \pm 1, \pm 3 \ldots$. Hence, transitions between K-ladders are now allowed. Water also has para and ortho states, characterized by antiparallel and parallel nuclear spins. The nuclear para states have either K_a or K_c odd while the ortho states have K_a and K_c either both even or both odd.

3.2.5 Hyperfine Transitions

The rotational spectra of many astrophysically relevant molecules contain hyperfine splittings due to electric quadrupole and magnetic dipole interactions with atoms with nonzero nuclear spin, such as ^{13}C, ^{14}N, and ^{17}O. The nuclear spin, $\vec{I}$, will couple with the rotational angular momentum, $\vec{J}$ to $\vec{F} = \vec{I} + \vec{J}$. The number of hyperfine levels is the smaller of $2J+1$ and $2I+1$. This is most relevant for nitrogen-bearing molecules and levels with $J > 0$ are split in to three hyperfine transitions. The relative intensities of the hyperfine transitions of a molecular transition can be calculated and the reader should consult a specialized book on this topic.

3.2.6 Λ Doubling

Some species have nonzero electronic angular momentum and this can couple to the rotations of the molecule. This has an effect on the molecular spectrum. We will focus here on

https://doi.org/10.1017/9781316718490.004 Published online by Cambridge University Press

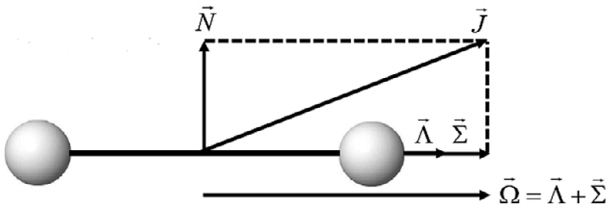

Figure 3.5 Λ-doubling of rotational levels in diatomic molecules. $\vec{N}$ is the nuclear rotational vector. $\vec{\Lambda}$ is the projection of the orbital angular momentum on the internuclear axis. $\vec{\Sigma}$ is the projection of $\vec{S}$ on the internuclear axis. $\vec{\Omega}$ is the vectorial sum of the latter two. When $\Lambda \neq 0$, the net current creates a magnetic field that can couple with the spinning electrons, splitting the energy levels.

a diatomic molecule with weak spin–orbit coupling and nonzero electron spin S. As discussed in Section 3.4.2, the term symbol for diatomic molecules is given by ${}^{2S+1}\Lambda_{\Omega}$ with $\vec{S}$ the total electron spin, $\vec{\Lambda}$ the projection of the orbital angular momentum on the internuclear axis, $\vec{\Sigma}$ the projection of $\vec{S}$ on the internuclear axis, and $\vec{\Omega} = \vec{\Sigma} + \vec{\Lambda}$ (Figure 3.5). The whole electronic shell can be considered to rotate around the molecular z axis. For a rotating molecule, we have the angular momentum of the rotation perpendicular to the z-axis, $\vec{N}$, and the total angular momentum of the electrons – composed of the orbital angular momentum, $\vec{L}$, and the spin angular momentum, $\vec{S}$ – precessing around the z-axis. The projections of the electronic components add to the total value (which is conserved), $\Omega\hbar = (\Lambda + M_s)\,\hbar$. As Ω is not zero, the total angular momentum of the molecule, J, is no longer perpendicular to the z-axis and the molecule will rotate around the space-fixed direction of $\vec{J}$.

The rotating molecule is then a symmetric top with the two moments of inertia, I_e, of the electrons rotating around the z-axis and I_m of atoms and electrons rotating around an axis perpendicular to the z-axis, with $I_e \ll I_m$. The rotational energy is then,

$$E_{rot} = \frac{J_x^2}{2I_x} + \frac{J_y^2}{2I_y} + \frac{J_z^2}{2I_z}. \tag{3.24}$$

We have $J_z^2 = \Omega^2\hbar^2$ and $J_x^2 + J_y^2 = J^2 - J_z^2 = \left(J\,(J+1) - \Omega^2\right)\hbar^2$ where we have made the classical to quantum replacement. This results in,

$$\frac{E_{rot}}{hc} = B_e\left(J\,(J+1) - \Omega^2\right) + A\Omega^2, \tag{3.25}$$

with the molecular rotational constant, $B_e = h/\left(8\pi^2 c I_m\right)$, and the electronic rotational constant, $A = h/\left(8\pi^2 c I_e\right)$. The latter term in the expression for the rotational energy does not depend on the rotation itself and is added to the electronic energy of the state Ω.

Generally, ground states of diatomic molecules are ${}^1\Sigma$ states with $\Omega = 0$ and we recover expression (3.5). But, as an example, consider OH with the electronic ground state ${}^2\Pi$ ($L = 1$ and $S = 1$) (Figure 3.6). Spin–orbit coupling provides then two sets of states

https://doi.org/10.1017/9781316718490.004 Published online by Cambridge University Press

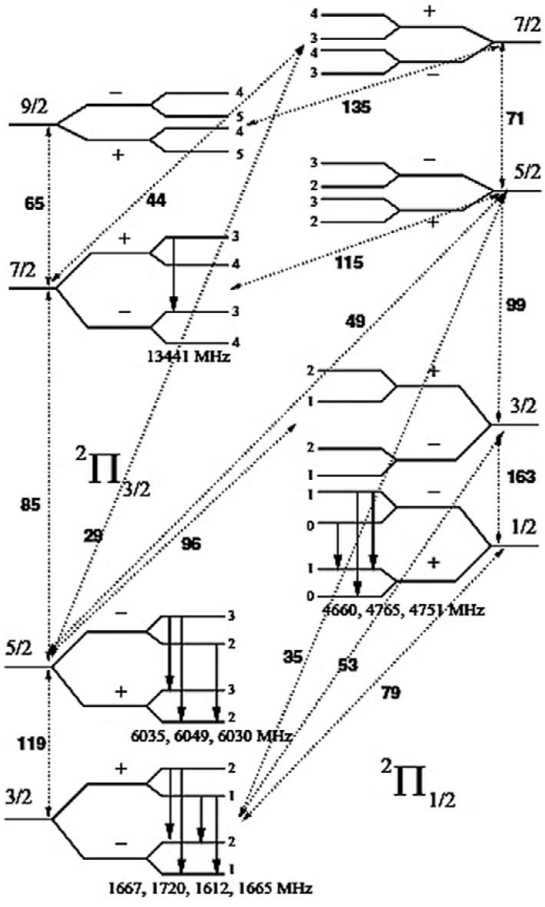

Figure 3.6 The rotational ladder of OH is split into two ($^2\Pi_{1/2}$ and $^2\Pi_{3/2}$) by spin–orbit coupling. Lambda doubling splits each level into half of opposite parity and hyperfine splitting results then in a total of four levels per J, labeled by the quantum number F. Splittings are not to scale. Known maser transitions (see Chapter 11) are indicated by solid arrows and labeled in MHz while relevant, pumping IR transitions are in μm. Figure taken from [10]

characterized by the electron orbital angular momentum, 1/2 and 3/2 ($\vec{J'} = \vec{L} + \vec{S}$), each containing a set of rotational ladders characterized by the rotational motion of the nuclei, J. Weak coupling between the electronic angular momentum and molecular angular momentum leads to lambda doubling of the rotational levels, depending on whether both are rotating in the same or in opposite sense. These Λ-doubles are then further split by coupling between the spin of the unpaired electron and the proton. These hyperfine levels have either parallel or antiparallel spins and are described by the total angular momentum quantum number, $F = J \pm I$. Each Λ-doublet can thus generate four lines; the transitions in which F does not change are called main lines. The other two are the satellite lines.

https://doi.org/10.1017/9781316718490.004 Published online by Cambridge University Press

A magnetic field will split the $2F + 1$ states of each hyperfine level further, leading to a set of complex transitons with different polarization characteristics. Allowed transitions require a parity change and $\Delta F = 0, \pm 1$ but $F = 0 \rightarrow 0$ is forbidden.

In summary, for OH, the two possible orientations of the spin angular momentum relative to the internuclear axis give rise to multiplet splitting into $^2\Pi_{3/2}$ and $^2\Pi_{1/2}$ systems separated by approximately 140 cm^{-1}. The interaction between the electronic orbital motion and the nuclear rotation splits each rotational level into two spin doublet levels and this lambda doubling is of order $0.1-1$ cm^{-1}. Finally, each lambda-doublet component is doubled due to the contribution of the nuclear spin in its interaction with the electronic plus rotational motion with a separation of approximately 10^{-3} cm^{-1} (Figure 3.6).

3.2.7 Nuclear Spin: Statistical Weight and Ortho and Para Species

The rotational degeneracy factor, g_J, reflects the possible projections of the angular momentum vector on a spatial axis and equals, $g_J = 2J + 1$ (as m_j ranges from $-J, \ldots, 0, \ldots, J$). In addition, the statistical weight of rotational levels includes the statistical weight of the nuclei, g_n, given by

$$g_n = \frac{1}{\sigma} \prod_n (I_n + 1), \tag{3.26}$$

where I_n is the spin of nucleus n and the product runs over all nuclei. The factor σ – part of the rotational partition function – takes the symmetry of the molecule into account (c.f. Section 3.2.8). Nucleons are fermions and have an intrinsic spin, $1/2$. The statistical weight of the nucleus can then be determined from the number of protons and neutrons. If the number of protons and neutrons are both even then the nucleus has no spin. If they are both odd then the nucleus has integer spin. If the number of protons plus the number of neutrons is odd, then the nuclear spin is 1/2. So, H, N, C, O have $I_n = 1/2, 1, 0, 0$, respectively. For relevant isotopes, we have D, ^{15}N, ^{13}C, ^{17}O, ^{18}O, equals $I_n = 1, 1/2, 1/2, 5/2, 0$. The statistical weight is then given by,

$$g\,(J) = g_n\,(2J + 1)\,. \tag{3.27}$$

Many molecular species come in para and ortho species, which differ in their nuclear spins (para with antiparallel nuclear spins and ortho with parallel nuclear spins). The presence of separate para and ortho species is a direct consequence of the generalized Pauli principle: Wavefunctions have to be antisymmetric with respect to the exchange of two fermions (particles with half-integral spin) and symmetric with respect to exchange of two bosons (particles with integral spin). The total wavefunction is (approximately) the product of the electronic, vibrational, rotational, and nuclear wavefunctions, $\psi_{tot} = \psi_e \psi_v \psi_r \psi_n$. As an example, consider H_2 with a ground electronic state $^1\Sigma_g^+$, which is symmetric with respect to the exchange of the nuclei. The vibrational wave function depends only on the internuclear distance and is thus symmetric as well. This implies that product of the rotational and nuclear spin wavefunctions has to be antisymmetric.

https://doi.org/10.1017/9781316718490.004 Published online by Cambridge University Press

Consider first the nuclear spin wavefunction. H atoms are fermions with $m_s = \pm 1/2$ (e.g. α and β). We have then four possible combinations for the two nuclei, 1 and 2: $\alpha\,(1)\,\alpha\,(2)$ and $\beta\,(1)\,\beta\,(2)$ and the two linear combinations, $(\alpha\,(1)\,\beta\,(2) + \alpha\,(2)\,\beta\,(1))\,/\,\sqrt{2}$ and $(\alpha\,(1)\,\beta\,(2) - \alpha\,(2)\,\beta\,(1))\,/\,\sqrt{2}$. The first three of these wavefunctions are symmetric with respect to exchange of the two nuclei. The latter is antisymmetric.

As mentioned above, we have to combine the symmetry of these states with those of the rotational states. The rotational wavefunction boils down to spherical harmonics, $Y_{J,M_J}\,(\theta,\phi)$, with J and M_J the rotational quantum numbers. Exchange of the two nuclei corresponds to a rotation by π and the symmetry properties of associated Legendre polynomials are given by $P\,(\pi - \theta) = (-1)^J\;P\,(\theta)$. Thus, even-$J$ levels are symmetric and have to combine with antisymmetric nuclear spin states, while odd-J levels are antisymmetric and have to combine with symmetric nuclear spin states to yield overall antisymmetric states.

This is also reflected in the statistical weight. Thus, for homonuclear diatomic molecules, with atomic spins, I_n, we have two sequences of statistical weights for rotational levels with J values differing in parity. The nuclear spin function is then given by, $g_n = g_n\,(i)$, according to Table 3.2, and,

$$g_n\,(1) = \frac{1}{2}[(2I_n + 1)^2 - (2I_n + 1)] \tag{3.28}$$

$$g_n\,(2) = \frac{1}{2}[(2I_n + 1)^2 + (2I_n + 1)] \tag{3.29}$$

Thus, for H_2 ($^1\Sigma_g^+$), we have $I_n = 1/2$ and for even (para) states, we have $g_n = 1$ while, for odd (ortho) states, we have $g_n = 3$. Half of the rotational states belong to the ortho form and half belong to the para form. The sum of the g_n's equals $(2I_n + 1)^2$.

Transitions between para and ortho states involve a change in nuclear spin and are thus forbidden. In terms of electro-magnetic allowed transitions, ortho and para forms are therefore "separate" species and, in space, exchange between them requires chemical reactions (e.g. $H_2 + H_3^+ \rightarrow H_2 + H_3^+$) or interaction with paramagnetic impurities (e.g. the lone electron pair on an oxygen atom) on a grain surface.

Table 3.2 *Nuclear spin statistical weight*[a]

Electronic state Indices	+ g	− u	− g	+ u
Even J	$g_n\,(1)$	$g_n\,(1)$	$g_n\,(2)$	$g_n\,(2)$
Odd J	$g_n\,(2)$	$g_n\,(2)$	$g_n\,(1)$	$g_n\,(1)$

[a] For Fermi-Dirac statistics. For Bose-Einstein statistics, the entries for even and odd J in the same column are interchanged. The first two rows specify the symmetry of the electronic states (see Section 3.4). The last two rows indicate which function to use for even and odd J with the electronic state specified in the same column (Eq. (3.28)).

https://doi.org/10.1017/9781316718490.004 Published online by Cambridge University Press

As another example, consider molecular oxygen, $^{16}O_2$, where each atom is a boson with $I_n = 0$. The electronic wavefunction of the ground state is asymmetric ($^3\Sigma_g^-$). Hence, the even J rotational states (and asymmetric nuclear spin states) have a weight equal to 0 and are missing in the spectra. The odd J states have a weight 1. In contrast, $C^{16}O_2$ has a symmetric ground electronic state ($^1\Sigma_g^+$). And now the symmetric rotational states couple with the symmetric nuclear spin states and have weight 1 while the asymmetric rotational states couple with the asymmetric spin states and have weight 0 and hence do not appear in the rotational spectra. Some other examples are, C_2H_2 with even (para) states and $g_n = 1$ and odd (ortho) states and $g_n = 3$. For water and formaldehyde, ortho and para states also have a ratio of the nuclear spin degeneracies of 3. For ammonia, we have two distinct species with ortho states with $K = 3n$ ($n = 0, 1, 2, \ldots$) and all spins parallel (3/2) and para states with $K \neq 3n$ and all spins not parallel (1/2). The ratio of the nuclear spin degeneracy factors is then 1.

3.2.8 Partition Function

Level populations are often expressed in terms of an excitation temperature (c.f. Sections 4.1.3, 4.2.1, and 4.2.2). In local thermodynamic equilibrium, we have for the level population, $n(J)$,

$$\frac{n(J)}{n} = \frac{g_J}{Z_r(T)} \exp\left[-E(J)/kT\right], \tag{3.30}$$

with T the temperature, $E(J)$ and g_J the energy and statistical weight of level J, and n the total density of the species. The rotational partition function, $Z_r(T)$, is given by,

$$Z_r(T) = \sum_J g_J \exp\left[-E(J)/kT\right]. \tag{3.31}$$

In this, the statistical weight factor includes the nuclear spin and hyperfine splitting factors. The rotational degeneracy factor reflects the projection on a spatial axis and equals, $2J + 1$ (cf. Section 3.2.7). For symmetric top molecules, the K states (except for $K = 0$) are doubly degenerate and hence have a factor $g_K = 2$ in their rotational statistical weight.

For high temperatures, the summation can be replaced by an integral. These can be evaluated for rigid rotors. For a linear molecule, the partition function becomes,

$$Z_r(T) = \frac{1}{\sigma} \frac{kT}{hcB}. \tag{3.32}$$

Nonlinear molecules can rotate around three major axes and the partition function is,

$$Z_r(T) = \frac{\sqrt{\pi}}{\sigma} \left(\frac{1}{ABC}\right)^{1/2} \left(\frac{kT}{hc}\right)^{3/2}. \tag{3.33}$$

These approximations are only valid if $kT/A, kT/B, kT/c \gg 1$. In these expressions, σ is a molecule-dependent symmetry factor. To understand this factor, consider a homonuclear diatomic molecule. Rotation by 180° does not change the molecule. Hence, we are overcounting the number of states by a factor 2. In general, we have to correct the partition

https://doi.org/10.1017/9781316718490.004 Published online by Cambridge University Press

Table 3.3 *Characteristics of molecular rotational transitions*

Species	Transition	ν_{ul} [GHz]	E_u [K]	A_{ul} [s^{-1}]	n_{cr} [cm^{-3}]
CO	1–0	115.3	5.5	7.2×10^{-8}	1.1×10^{3}
	2–1	230.8	16.6	6.9×10^{-7}	6.7×10^{3}
	3–2	346.0	33.2	2.5×10^{-6}	2.1×10^{4}
	4–3	461.5	55.4	6.1×10^{-6}	4.4×10^{4}
	5–4	576.9	83.0	1.2×10^{-5}	7.8×10^{4}
	6–5	691.2	116.3	2.1×10^{-5}	1.3×10^{5}
	7–6	806.5	155.0	3.4×10^{-5}	2.0×10^{5}
CS	1–0	49.0	2.4	1.8×10^{-6}	4.6×10^{4}
	2–1	98.0	7.1	1.7×10^{-5}	3.0×10^{5}
	3–2	147.0	14	6.6×10^{-5}	1.3×10^{6}
	5–4	244.9	35	3.1×10^{-4}	8.8×10^{6}
	7–6	342.9	66	1.0×10^{-3}	2.8×10^{7}
	10–9	489.8	129	2.6×10^{-3}	1.2×10^{8}
HCO^+	1–0	89.2	4.3	3.0×10^{-5}	1.7×10^{5}
	3–2	267.6	26	1.0×10^{-3}	4.2×10^{6}
	4–3	356.7	43	2.5×10^{-3}	9.7×10^{6}
HCN	1–0	88.6	4.3	2.4×10^{-5}	2.6×10^{6}
	3–2	265.9	26	8.4×10^{-4}	7.8×10^{7}
	4–3	354.5	43	2.1×10^{-3}	1.5×10^{8}
H_2CO	2_{12}–1_{11}	140.8	6.8	5.4×10^{-5}	1.1×10^{6}
	3_{13}–2_{12}	211.2	17	2.3×10^{-4}	5.6×10^{6}
	4_{14}–3_{13}	281.5	30	6.0×10^{-4}	9.7×10^{6}
	5_{15}–4_{14}	351.8	47	1.2×10^{-3}	2.6×10^{7}
NH_3	(1,1) inversion	23.7	1.1	1.7×10^{-7}	1.8×10^{3}
	(2,2) inversion	23.7	42	2.3×10^{-7}	2.1×10^{3}
H_2	2–0	1.06E4[a]	510	2.9×10^{-11}	10
	3–1	1.76E4[b]	1015	4.8×10^{-10}	300

[a] λ = 28.2 μm. [b] λ = 17.0 μm.

function by the (symmetry) factor equal to the distinct number of ways in which rotation brings a molecule into equivalent configurations. These symmetry factors can be evaluated through group theory but that is beyond the scope of this book. Simple symmetry considerations often suffice to show that, e.g., CH_4 has $\sigma = 12$.

We can define characteristic rotational temperature, $\theta_r = hcB/k$, and values for some astrophysically interesting species are summarized in Table 3.4.

3.2.9 Transition Strength

The excitation and deexcitation of molecular levels is described by the Einstein coefficients: The Einstein A_{ul} is the rate of spontaneous emission between an upper (u) and lower (l)

https://doi.org/10.1017/9781316718490.004 Published online by Cambridge University Press

Table 3.4 *Characteristic rotational and vibrational temperatures*[1]

Species	Mode	θ_v [K]	θ_r [K]	Species	Mode	θ_v [K]	θ_r [K]
H_2	ν_1	6330	88	CO_2	ν_1	3360	0.561
CH_4	ν_1	4170	7.54		ν_2	954 (2)	
	ν_2	2180 (2)	7.54		ν_3	1890	
	ν_3	4320 (3)	7.54	CH_3OH	ν_1	5297	6.125
	ν_4	1870 (3)			ν_2	4315	1.185
NH_3	ν_1	4800	13.6		ν_3	4092	1.141
	ν_2	1360	13.6		ν_4	2125	
	ν_3	4880 (2)	8.92		ν_5	2093	
	ν_4	2330 (2)			ν_6	1928	
H_2O	ν_1	5360	40.1		ν_7	1546	
	ν_2	2290	20.9		ν_8	1487	
	ν_3	5160	13.4		ν_9	2834	
H_2CO	ν_1	4003	13.53		ν_{10}	2108	
	ν_2	2512	1.864		ν_{11}	1647	
	ν_3	2158	1.632		ν_{12}	389	
	ν_4	4091		CO	ν_1	3122	2.78
	ν_5	1797					
	ν_6	1679					

[1]Temperatures θ are expressed as $h\nu/k$ and hcB/k. Numbers in brackets indicate the degeneracy of the mode.

level. The Einstein B_{lu} coefficient is the absorption rate between these two levels while the B_{ul} coefficient is the rate of stimulated emission. For a two-level system controlled by radiation, the level populations are given by,

$$B_{lu} J_{ul} n_l = (A_{ul} + B_{ul} J_{ul})\, n_u. \tag{3.34}$$

In thermodynamic equilibrium, the level populations are given by the Boltzmann equation, $n_u/n_l = (g_u/g_l)\, \exp\left[-E_{ul}/kT\right]$ while the radiation field is given by Planck's law, $J_{ul} = B\,(\nu_{ul}) = 2h\nu_{ul}^3/c^2\, \left(\exp\left[h\nu_{ul}/kT\right] - 1\right)^{-1}$ where $E_{ul} = h\nu_{ul}$. Combining these equations gives rise to the well-known relationships between the Einstein coefficients,

$$g_u B_{ul} = g_l B_{lu} \tag{3.35}$$

$$A_{ul} = (2h\nu_{ul}^3/c^2)\, B_{ul}. \tag{3.36}$$

As the Einstein coefficients are properties of the species involved, they must be valid even when the system is not in thermodynamic equilibrium. In terms of the Einstein coefficients, the energy emitted is given by $j_{ul} = A_{ul} n_u h\nu_{ul}/4\pi$ and the energy absorbed from a pencil ray, corrected for stimulated emission, is given by, $\kappa_{lu} = (n_l B_{lu} - n_u B_{ul})\, h\nu_{ul}/4\pi$. In terms of the oscillator strength, f, the Einstein B coefficient is given by,

https://doi.org/10.1017/9781316718490.004 Published online by Cambridge University Press

$$B_{lu} = \frac{4\pi}{h\nu_{ul}} \frac{\pi e^2}{m_e c} f_{lu}, \tag{3.37}$$

with m_e the mass of the electron.

Let us consider now the transition strength. A rotating dipole will emit an electromagnetic wave and the average power radiated is given by Larmor's formula,

$$\langle P \rangle = \frac{64\pi^4}{3c^3} \nu^4 \, |\mu_{ul}|^2, \tag{3.38}$$

with μ_{ul} the mean electric dipole moment associated with the transition. The Einstein A_{ul} is then,

$$A_{ul} = \frac{64\pi^4}{3hc^3} \nu^3 \, |\mu_{ul}|^2 \tag{3.39}$$

For a rotational transition, the dipole moment can be expressed as,

$$|\mu_{ul}|^2 = \mu_z^2 \frac{S_{ul}}{g_u}, \tag{3.40}$$

with μ_z the electric dipole moment along the molecular symmetry axis. The distribution of the line intensity over the different rotational bands is represented by the line strength of the transition, S_{ul}, the so-called Hönl–London factor. The calculation of the line strength can be quite complex. For linear molecules in the ground vibrational state, we have,

$$|\mu_{ul}|^2 = \mu_d^2 \frac{J+1}{2J+3}, \tag{3.41}$$

with μ_d the molecule's permanent dipole moment. For symmetric top molecules, we have,

$$|\mu_{ul}|^2 = \mu_d^2 \frac{J^2 - K^2}{2J+3}. \tag{3.42}$$

The $2J + 3$ factor in these expressions is the statistical weight of the upper level. Hence, when $J \gg 1$, we have $|\mu_{ul}|^2 \simeq \mu_d^2$. The transition probability increases rapidly with ν and hence with J; for a linear molecule, $A \propto (J+1)^4 / (2J+3)$. Which for large J simplifies to $\propto J^3$.

Recapping these results. The Einstein A scales with ν^3 times the transition dipole moment. The Einstein B scales with the transition dipole moment. The oscillator strength and absorption coefficient scale with the transition dipole moment times ν. In addition to these frequency dependencies, we also have to recognize the effect of mass of the particles on the intrinsic strength of transitions alluded to in Section 3.1. Finally, independent of this, when transitions are dipole forbidden, electric quadrupole or magnetic dipole transitions are a factor α^2 weaker with α the fine-structure constant (1/137).

Table 3.3 summarizes the characteristics of rotational transitions of some astrophysically relevant molecules. We note that homonuclear diatomic molecules (e.g. H_2, O_2, N_2), some symmetric, linear, heteronuclear molecules (e.g. CO_2, CS_2), some symmetric top molecules

https://doi.org/10.1017/9781316718490.004 Published online by Cambridge University Press

(e.g. C_6H_6), and spherical top molecules (e.g. CH_4) have no permanent dipole and, hence, no allowed rotational transitions. These species can still have magnetic dipole allowed transitions.

3.3 Vibrational Spectroscopy

3.3.1 Energy Levels

When a molecule vibrates, it may undergo a change in dipole moment and it will, then, couple to an electromagnetic field. Consider a diatomic molecule and small vibrations around an equilibrium position. The potential energy is then a quadratic function of the vibrational coordinates, and the essence of vibrational spectroscopy is then contained within Hooke's law for a harmonic oscillator,

$$\nu = \frac{1}{2\pi\, c}\sqrt{\frac{\kappa}{\mu}}, \tag{3.43}$$

with ν the fundamental frequency, κ the force constant, μ the reduced mass of the molecular units vibrating, and the factor c is included to transform the unit to wavenumbers (cm^{-1}) for cgs units, commonly used in spectroscopy. Molecular bond strengths are, of course, very similar to binding energies of electrons to an atom. However, the frequencies of the transitions of molecular vibrational levels are, thus, shifted to lower energies by $\sqrt{m_e/M}$, with m_e and M the mass of the electron and atom, respectively, and occur in the near- and mid-IR.

Real molecules are not harmonic oscillators and, as a result of anharmonicity of the bonding, hot bands (e.g. 2-1, 3-2) are generally shifted to lower frequencies. A Morse potential is a convenient description of the interaction of a diatomic molecule,

$$V(R) = D_e\left(\exp\left[-2a\left(R - R_e\right)\right] - 2\exp\left[-a\left(R - R_e\right)\right]\right), \tag{3.44}$$

where R and R_e are the internuclear distance and equilibrium distance, and D_e is the dissociation energy, and a equals,

$$a = \nu_e\sqrt{\mu/2D_e}, \tag{3.45}$$

with ν_e the fundamental frequency. We recognize the short range repulsive and long range attractive forces in equation (3.44). The Schrödinger equation can be solved exactly for the Morse potential, and the energy levels are,

$$E(v) = h\nu_e\left(v + 1/2\right) - h\nu_e x_e\left(v + 1/2\right)^2, \tag{3.46}$$

with $x_e\nu_e = \nu_e^2/4D_e$ the anharmonicity constant. The $1/2$ term accounts for the zero-point energy and implies that even when the molecule has no vibrational excitation, the atoms are still vibrating, in accordance with Heisenberg's uncertainty principle. The Morse

https://doi.org/10.1017/9781316718490.004 Published online by Cambridge University Press

potential has a maximum number of levels, $v_{max} \simeq 2D_e/\nu_e$. The frequencies of vibrational transitions are then,

$$\nu\,(v) = \nu_e - 2\nu_e x_e\ (v+1)\,. \tag{3.47}$$

Now consider a polyatomic molecule and again study small vibrations around an equilibrium position that are represented by quadratic potentials. This results in a set of uncoupled harmonic oscillators. The total energy is then given by,

$$E = E_0 + \sum_k v_k h\nu_k, \tag{3.48}$$

with v_k and ν_k the vibrational quantum number and frequency of mode k. The zero-point energy, E_0, is given by,

$$E_0 = \frac{1}{2}\sum_k h\nu_k. \tag{3.49}$$

Anharmonicity – due to electronic repulsion at short distances, and dissociation at large distances – will play an important role. In polyatomic molecules, diagonal terms depend on the coordinates of a single oscillator while off-diagonal terms will link different oscillators and the energy (Eq. (3.48)) will contain cross terms. In principle, there are then $N_m\,(N_m+1)\,/2$ anharmonicity constants for a molecule with N_m normal modes.

For a molecule, translational degrees of freedom have been converted into vibrational and rotational degrees of freedom. In the harmonic approximation, the motions of the atoms in the molecule can be decomposed into the normal modes of vibration, which are linearly independent motions (i.e. mutually orthogonal). A molecule with N atoms will have $3N$ degrees of freedom, but three of those are associated with translational motion and three (two for linear molecules) with rotations, leaving $3N-6$ ($3N-5$) vibrational modes. These modes will differ in their force constants and reduced mass and, hence, will occur at different frequencies. Some of the $3N-6$ modes may occur at the same frequency and hence these modes are degenerate. For N_{dg} degenerate modes, we have $n_v = 3N-5-N_{dg}$ for linear molecules and $n_v = 3N-6-\sum_{k=1}^{k=N_{dg}}(d_n-1)$ for nonlinear molecules with d_n the degeneracy of the nth mode. In principle, all atoms are moving for a given normal mode. However, it is sometimes advantageous to "classify" these modes as stretching (symmetric and asymmetric) and bending (scissoring, rocking, wagging, and twisting) vibrations of specific atoms (or groups of atoms) in the molecule. This can be particularly advantageous for CH stretching modes as these are relatively isolated. Thinking in terms of local modes can also be insightful when considering vibrations near the dissociation limit.

Modes will be infrared-active if the dipole moment changes during the vibration. Conversely, some vibrations can be infrared inactive; e.g. the symmetric stretching vibrations in C_2H_2. The symmetry of a mode is described using group theory and this is used to determine whether a mode is IR and/or raman active. Group theory is beyond the scope of this book. In general, the absorption strength will be stronger for more polar bonds.

https://doi.org/10.1017/9781316718490.004 Published online by Cambridge University Press

Numbering of vibrational modes is governed by symmetry type set by group theory: Start with the completely symmetric modes and sort them by wavenumber. This yields the numbering of these modes. Do the same with subsequent symmetry types. In this, nondegenerate modes are numbered before degenerate modes. Degenerate modes receive the same number but are recognized by a superscript.[2] There is one (historical) exception: the bending modes of linear triatomic molecules is always labeled, ν_2. As an example, methane has nine fundamental modes: the symmetric stretch ($\nu_1 = 2917\ \mathrm{cm}^{-1}$), the doubly degenerate deformation mode ($\nu_2 = 1534\ \mathrm{cm}^{-1}$), the triply degenerate stretch ($\nu_3 = 3019\ \mathrm{cm}^{-1}$), and the triply degenerate deformation mode ($\nu_4 = 1306\ \mathrm{cm}^{-1}$). Only the ν_3 and the ν_4 modes are IR active. Vibrations in homonuclear molecules do not lead to changes in the dipole moment and hence are infrared inactive. Mixing of isotopes in such species will lead to infrared absorptions as the center of mass and the center of charge no longer coincide. Likewise, interactions with the environment in a solid will introduce weak infrared activity.

Anharmonicity introduces small shifts in the frequencies of the species. In addition, overtones ($\Delta v > 1$) become allowed. Besides these fundamentals, we can also expect combination bands (i.e. $\nu_i + \nu_j$ with $\Delta v_i = \Delta v_j = 1$ or $2\nu_i + \nu_j$ with $\Delta v_i = 2$, $\Delta v_j = 1$, etc.) and difference bands (i.e. $\nu_i - \nu_j$ with $\Delta v_i = \pm 1$ and $\Delta v_j = \mp 1$). In general, fundamental bands are much stronger than overtones or combination/difference bands. However, this can change due to resonance interaction. The near (accidental) resonances between a fundamental and an overtone/combination/difference band of the same symmetry will lead to mixing of the states. This will shift the frequencies of the modes away from each other and the weaker mode will borrow intensity from the stronger mode.

3.3.2 Partition Function

In general, the statistical weight of vibrational levels is $g_v = 1$ but, for degenerate modes, this has to be modified. The total vibrational statistical weight, including degeneracy, of the state, $\{v_1, v_2, v_3, \dots\}$, is given by

$$g_{v_1, v_2, v_3, \dots} = \sum_{k=1}^{k=n_v} \frac{(v_n + d_n - 1)!}{v_n!\,(d_n - 1)!}, \tag{3.50}$$

where each term represents the different way v_n quanta can be distributed over d_n (degenerate) modes. For a doubly degenerate vibration, this becomes $v_n + 1$, while for a triply degenerate vibration, we have $(v_n + 1)(v_n + 2)/2$.

For a single mode, the vibrational partition function is given by,

$$Z_{vib}(T) = \sum_{v} \exp\left[-E_{vib}(v)/kT\right], \tag{3.51}$$

[2] The bending mode of a linear polyatomic molecule is degenerate as the molecule can bend in the $x - z$ and/or $y - z$ plane. The two oscillators in the x and y direction are combined to yield circular motion and ℓ is the quantum number associated with this vibrational angular momentum. Level, v, in this mode has degeneracy $v + 1$ ($|\ell| = v, v - 2, \dots 0$ or 1; + and − signs correspond to clockwise and anticlockwise rotation).

https://doi.org/10.1017/9781316718490.004 Published online by Cambridge University Press

with $E_{vib}(v)$ the vibrational energy of level v of this mode. Ignoring anharmonic interaction, the partition function of a polyatomic molecule is given by the product of the vibrational partition function of each normal mode. For a single harmonic oscillator and measuring the energy relative to the zero-point energy, we have, $E_{vib} = vh\nu_e$, and

$$Z_{vib}(T) = \sum_v \left(\exp\left[-h\nu_e/kT\right]\right)^v = \left(1 - \exp\left[-h\nu_e/kT\right]\right)^{-1}. \tag{3.52}$$

Including degeneracy, this becomes,

$$Z_n(T) = \left(1 - \exp\left[-h\nu_e/kT\right]\right)^{-d_n}. \tag{3.53}$$

The total vibrational partition frunction is then,

$$Z_{vib}(T) = \prod_{k=1}^{n_v} \left(1 - \exp\left[-h\nu_e/kT\right]\right)^{-d_n}. \tag{3.54}$$

We can define characteristic vibrational temperatures as $\theta_v = h\nu_e/k$ and values for some astrophysically relevant species are summarized in Table 3.4. Typically, $\theta_v/T \ll 1$ and $Z_{vib} \simeq 1$ for a mode and hence, in essence, only the ground state is populated. However, large molecules have many, many modes and even if for each mode the vibrational partition function is close to 1, the product is still a large factor. Moreover, when excitation temperatures are high, partition functions can quickly become astronomically large. We will return to this in Chapter 8.3, where we discuss the excitation of large molecules.

3.3.3 Molecular Identification

Vibrational transitions are very characteristic for the motions of the atoms in the molecular group directly involved in the vibration but much less sensitive to the structure of the rest of the molecule. Characteristic band positions of various molecular groups are illustrated in Figure 3.7 and summarized in Table 3.5. Modes involving motions of hydrogen occur

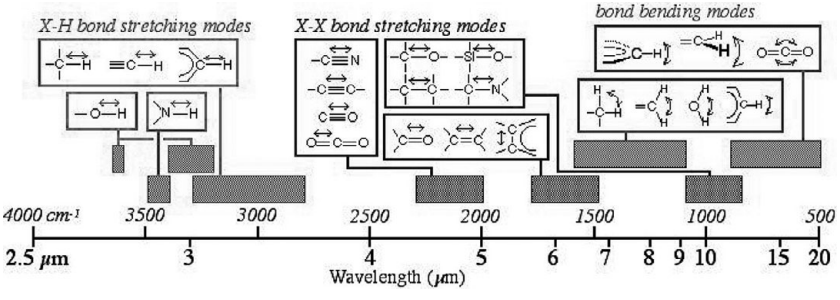

Figure 3.7 Summary of the vibrational frequencies of various molecular groups. The boxes indicate the range over which specific molecular groups absorb. The vibrations of these groups are schematically indicated in the linked boxes. Figure kindly provided by D. Hudgins

https://doi.org/10.1017/9781316718490.004 Published online by Cambridge University Press

Table 3.5 *Characteristic vibrational band positions*

Group	Mode	Frequency range [cm^{-1}]	Note
OH stretch			
	Free OH	3,610–3,645[a]	Sharp
	Intramolecular[b]	3,450–3,600	Sharp
	Intermolecular[c]	3,200–3,550	Broad
	Chelated[d]	2,500–3,200	Very broad
NH stretch			
	Free NH	3,300–3,500	Sharp
	H-bonded NH	3,070–3,350	Broad
CH stretch			
	≡C–H	3,280–3,340	
	=C–H	3,000–3,100	
	$CO–CH_3$	2,900–3,000	Ketones
	$C–CH_3$	2,865–2,885	Symmetric
		2,950–2,975	Asymmetric
	$O–CH_3$	2,815–2,835	Symmetric
		2,955–2,995	Asymmetric
	$N–CH_3$	2,780–2,805	Aliphatic amines
	$N–CH_3$	2,810–2,820	Aromatic amines
	CH_2	2,840–2,870	Symmetric
		2,915–2,940	Asymmetric
	CH	2,880–2,900	
C≡C stretch			
	C≡C	2,100–2,140	Terminal group
	C–C≡C–C	2,190–2,260	
	C–C≡C–C–C≡C–	2,040–2,200	
C≡N stretch			
	Saturated aliphatic	2,240–2,260	
	Aryl	2,215–2,240	
C=O stretch			
	Non-conjugated	1,700–1,900	
	Conjugated[e]	1,590–1,750	
	Amides	1,630–1,680	
C=C stretch			
	$–HC=C=CH_2$	1,945–1,980	
	–HC=C=CH–	1,915–1,930	
CH bend			
	CH_3	1,370–1,390	Symmetric
		1,440–1,465	Asymmetric
	CH_2	1,440–1,480	
	CH	1,340	

Continued

https://doi.org/10.1017/9781316718490.004 Published online by Cambridge University Press

Table 3.5 *Continued*

Group	Mode	Frequency range [cm^{-1}]	Note
CO–O–C stretch			
	Formates	~1,190	
	Acetates	~1,245	
C–O–C stretch			
	Saturated aliphatic	1,060–1,150	Asymmetric
	Alkyl,aryl ethers	1,230–1,277	
	Vinyl ethers	1,200–1,225	
Aromatic modes			
	C–H stretch	~3,030	
	C–H deformation	~1,160	In plane
	C–H deformation	900–740	Out of plane[f]
	C=C stretch	1,590–1,625, 1,280–1,315	

[a] The OH frequency of free water occurs at 3756 cm^{-1}. [b] H-bonded as dimer or polymer. [c] In a fully H-bonded network such as ice. [d] The OH is H-bonded to an adjacent C=O group. [e] Two double bonds separated by a single bond. [f] Pattern of bands whose position depends on number of adjacent C-atoms with H.

at considerably higher frequencies than modes involving similar motions of heavier atoms (again, Hooke's law, Eq. (3.43)). Thus, H-stretching vibrations occur in the 3 μm region, while stretching motions among (single bonded) C, N, and O atoms are located around 10 μm. Likewise, when the bond strength increases, the vibration shifts to higher frequencies and singly, doubly, and triply bonded CC vibrations shift from about 1000 to 2000 cm^{-1} (Figure 3.7).

Vibrational spectra can be used as fingerprints for the identification of the molecular groups of a species and, hence, provide a powerful tool to determine the class of molecules present (e.g. alkanes versus aldehydes). However, as a rule, vibrational spectra cannot easily distinguish the specific molecule within a class. The smallest molecule within a class often forms an exception to this rule. For example, the C–H stretching vibration of methane (3019 cm^{-1}) is shifted from that of other alkanes (2840–2975 cm^{-1}). For a pure substance, subtleties within the spectra can be used to identify the compound present. Thus, the spectrum of n-hexane (C_6H_{14}) will show absorptions at the positions of the stretching and bending vibrations of methyl (CH_3) and methylene (CH_2) groups in a relative strength commensurate with the intrinsic strength of the modes of these molecular groups and the relative number of CH_3 and CH_2 groups present in the molecule (2 versus 4 groups). The isomer isohexane (2-methylpentane with an additional methyl group replacing one of the H's on the second C-atom of the pentane molecule) will also show methyl and methylene absorptions but in a different relative strength (3 versus 3 groups). Furthermore, the methyl bands will be split due to interaction between the adjacent CH_3 groups. In the gas

https://doi.org/10.1017/9781316718490.004 Published online by Cambridge University Press

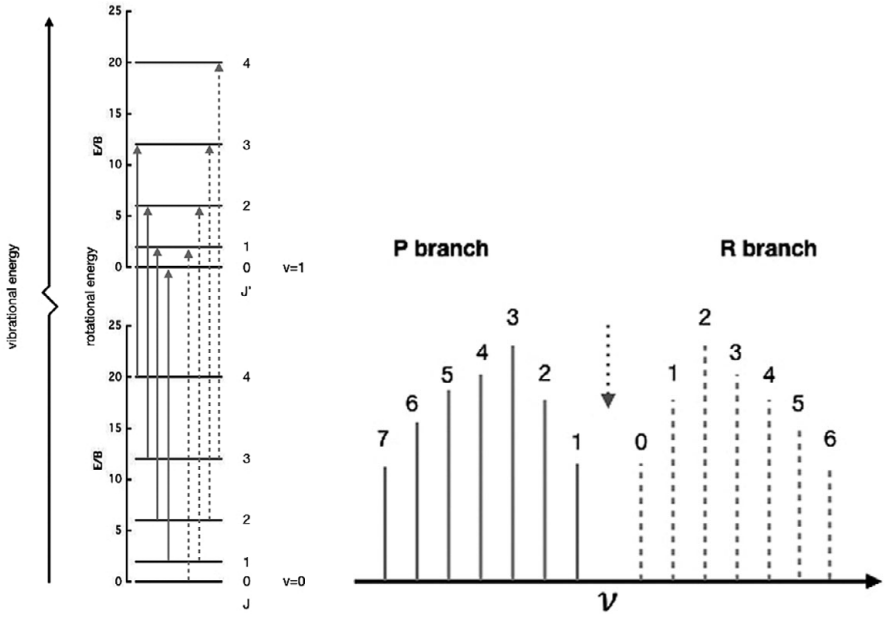

Figure 3.8 Ro-vibrational spectra of a diatomic rigid rotating harmonic oscillator. Left: Energy level diagram including the ground and first excited vibrational state and their associated rotational states. P-branch ($\Delta J = -1$) and R-branch ($\Delta J = +1$) transitions are indicated by full and dashed arrows. Q-branch ($\Delta J = 0$) transitions are missing. Right: The resulting spectrum consists of equidistant lines separated by $2B$ and centered around the fundamental frequency, ν. Q-branch transitions would pile up at ν. P and R branch transitions are labeled by the rotational quantum number from the level in the lower vibrational state. The relative strength of the transitions largely reflects the population distribution of the states involved. This will be discussed in Section 4.1.1.

phase, identification can be considerably aided by resolved P, Q, and R-branches (Section 3.3.4). In the solid state, when a mixture of species is present, identification of specific molecular species present within a class is often daunting.

3.3.4 Gas Phase Ro-vibrational Spectra

Molecules can vibrate and rotate simultaneously and that is reflected in the energy levels. For a diatomic molecule, we can write for the energy levels,

$$\frac{E}{hc} = \nu_e \left(v + \frac{1}{2}\right) - \nu_e x_e \left(v + \frac{1}{2}\right)^2 \tag{3.55}$$

$$+ B_e J\,(J+1) - D_e J^2\,(J+1)^2 - \alpha_e \left(v + \frac{1}{2}\right) J\,(J+1) \tag{3.56}$$

where the subscript e implies that the quantity is evaluated at the equilibrium position of the nuclei. The first two terms refer to vibrational energy levels of an anharmonic oscillator.

https://doi.org/10.1017/9781316718490.004 Published online by Cambridge University Press

The next two are the rigid rotor plus the centrifugal distortion. The last term gives the vibration–rotation interaction. The first four terms have been described in Sections 3.2 and 3.3. For a Morse potential, we can write for the rotation–vibration interaction constant,

$$\alpha_e = 6\sqrt{\frac{x_e B_e^3}{\nu_e}} - 6\frac{B_e^2}{\nu_e}. \tag{3.57}$$

Ignoring for the moment the rotation–vibrational interaction, we recognize that the total energy is the sum of the rotational and vibrational energy. The selection rules are the same as for the individual motions, $\Delta v = \pm 1$, $\Delta J = \pm 1$. Now consider the transition from $v = 1 \leftarrow 0$. Simple algebra shows that the transition frequency is

$$\nu_{v=0\rightarrow 1,\, J\rightarrow J'} = \nu_e\left(1 - 2x_e\right) + B_e\left(J - J'\right)\left(J + J' + 1\right) \tag{3.58}$$

$$- D_e\left(J^2\left(J+1\right)^2 - J'^2\left(J'+1\right)^2\right), \tag{3.59}$$

where we have assumed the same rotational constants in the upper and lower state and indicated the rotational levels as J' and J'' for $v = 1$ and $v = 0$, respectively. For $\Delta J = 1$ – the so-called R-branch[3] – we now have $J' - J'' = 1$ and,

$$\nu_{v=0\rightarrow 1,\, J\rightarrow J+1} = \nu_e\left(1 - 2x_e\right) + 2B_e\left(J+1\right) - 4D_e\left(J+1\right)^3 \tag{3.60}$$

and for $\Delta J = -1$ – the so-called P-branch[3],

$$\nu_{v=0\rightarrow 1,\, J\rightarrow J-1} = \nu_e\left(1 - 2x_e\right) - 2B_e J - 4D_e J^3. \tag{3.61}$$

Note that in these expressions, J stands for the rotational quantum number in the lower vibrational state. There is no line at the band center, $\nu = \nu_e\left(1 - 2x_e\right)$. When the centrifugal distortion is small, we can ignore the D_e terms and we have two branches of equally spaced lines separated by $2B_e$ appearing on either side of the line center with the P-branch on the lower frequency side. Note that for, e.g., H_2 the selection rules are $\Delta J = \pm 2$ and these transitions are labeled as O(J) and S(J).

The ro-vibrational coupling expresses that as the bond length increases in a higher vibrational state, the moment of inertia also increases. As a consequence, the rotational constant will be smaller (i.e. $B_v \rightarrow B_e - \alpha_e\left(v + 1/2\right)$). We can write,

$$\nu_R\left(J''\right) = \nu\left(v''\right)_0 + 2B'_v + \left(3B'_v - B''_v\right)J'' + \left(B'_v - B''_v\right)J''^2 \tag{3.62}$$

$$\nu_P\left(J''\right) = \nu\left(v''\right)_0 - \left(B'_v + B''_v\right)J'' + \left(B'_v - B''_v\right)J''^2, \tag{3.63}$$

where the double prime refers to the ground state and the single prime to the upper state. Note that $B'_v - B''_v < 0$ and the spacing in the P-branch will be larger than in R branch. Also, the P-branch spreads out while the R-branch bunches up with increasing rotational quantum number. The bunching up of the R branch leads to the formation of a bandhead, which we can quantify,

[3] For the P-, Q-, and R-branches, transitions are labeled as P(J), QP(J), R(J), respectively, with J the rotational quantum number of the level in the lower vibrational state.

https://doi.org/10.1017/9781316718490.004 Published online by Cambridge University Press

$$\frac{d\nu_R\left(J''\right)}{dJ} = \left(3B'_v - B''_v\right) + \left(B'_v - B''_v\right) J'' = 0. \tag{3.64}$$

This results in J'' (bandhead) $\simeq B_e/\alpha_e$. For CO, this is about 100.

Linear polyatomic molecules can be treated similar to diatomic molecules and their spectral patterns are the same. We can now recognize parallel bands where the vibration introduces a change in dipole moment along the molecular axis and perpendicular bands where the change in dipole moment is perpendicular to the molecular axis. For parallel bands, the selection rules are $\Delta v = 1$ and $\Delta J = \pm 1$ and transitions will show P and R branches. For perpendicular bands, the selection rules are $\Delta v = 1$ and $\Delta J = 0, \pm 1$. As the rotation–vibration constant is small, Q-branch[3] ($\Delta J = 0$) will occur at almost the same frequency but there is a small red shading as $\alpha_e < 0$. The amount of red shading is a function of the temperature.

For a symmetric top molecule, we have two rotational quantum numbers and two rotational constants. We can again recognize parallel and perpendicular bands now according to whether the change in dipole moment is parallel or perpendicular to the main axis of rotation of the molecule. The energy levels are (ignoring centrifugal distortion and rotational–vibrational coupling),

$$\frac{E}{hc} = \nu_e\left(v + \frac{1}{2}\right) - \nu_e x_e\left(v + \frac{1}{2}\right)^2 + B_e J\left(J+1\right) + \left(A - B\right) K^2. \tag{3.65}$$

The selection rules are $\Delta v = 1$, $\Delta J = \pm 1, 0$, and $\Delta K = 0$ (except for $K = 0$ where $\Delta J = \pm 1$) and there are P, Q, and R branches. For $K = 0$, the spectrum is that of a linear molecule without a Q-branch. In general, as I_A/I_B decreases, the intensity of the Q branch decreases. Consider first the parallel modes, which will have simple P, Q, and R branches except that – as for the pure rotational transitions – these split up into $J+1$ K-components at high spectral resolution. The perpendicular transitions are complicated by strong coriolis interaction. For a prolate and oblate top, the rotational energy levels are given as,

$$\frac{E}{hc} = BJ\left(J+1\right) + \left(A - B\right) K_A^2 \mp 2A\zeta K_A \tag{3.66a}$$

$$\frac{E}{hc} = BJ\left(J+1\right) + \left(C - B\right) K_C^2 \mp 2C\zeta K_C \tag{3.66b}$$

where ζ is the coriolis coupling constant.[4] The selection rules are $\Delta v = 1$, $\Delta J = \pm 1, 0$, and $\Delta K = \pm 1$. This large coriolis splitting shifts the K-structure and results in separate subbands ($K' \leftarrow K''$ transitions), where each subband has a P, Q, and R branch. The subbands' origins are approximately separated by $2\left(A\left(1-\zeta\right) - B\right)$. Depending on the magnitudes of A, B, and ζ these perpendicular subbands can be well separated or result in a massive congested spectra.

[4] The coriolis coupling constant, ζ, is the vibrational angular momentum but unlike for a linear molecule, ζ ($-1 \le \zeta \le 1$) is not necessarily an integer.

https://doi.org/10.1017/9781316718490.004 Published online by Cambridge University Press

Furthermore, the P and R branch will split because of a difference in $A - B$ between the upper and lower vibrational levels and the Q branch will split because of a difference between B in the upper and lower vibrational levels. For perpendicular bands, the selection rules are $\Delta v = 1$, $\Delta J = \pm 1, 0$, and $\Delta K = \pm 1$ and there are P, Q, and R branches. For the R branch, we have $\Delta J = +1$, $\Delta K = \pm 1$, and $\nu_R = \nu_o + 2B(J+1) + (A-B)(1 \pm 2K)$; for the P branch, we have $\Delta J = -1$, $\Delta K = \pm 1$, and $\nu_P = \nu_o - 2BJ + (A-B)(1 \pm 2K)$; for the Q branch, we have $\Delta J = 0$, $\Delta K = \pm 1$, and $\nu_Q = \nu_o + (A-B)(1 \pm 2K)$. Note that there are two sets of P, Q, and R branches for each lower state value of K.

For asymmetric top molecules, the spectra become very complex and have to be calculated numerically.

3.3.5 Accurate Line Lists

The potential of a molecule can be expanded into a Taylor series around the equilibrium position, which for a diatomic molecule reads as,

$$E(R) = \sum_n \frac{1}{n!} \left(\frac{\partial^n E}{\partial R^n} \right)_{R_e} (R - R_e)^n . \tag{3.67}$$

Such an approach can be the basis for the reproduction of the rotational–vibrational spectrum. The Dunham expansion is then often used for the term expansion,

$$E(v, J) = \sum_{k,l} Y_{k,l} \, (v + 1/2)^k \, (J(J+1))^l . \tag{3.68}$$

The coefficients, $Y_{k,l}$, in this expansion are then determined by comparison to experimental data. The first terms are readily assigned to ν_e & $-\nu_e x_e$ and B_e & D_e, and $-\alpha_e$ (cf. Eq. (3.46)) and can be linked to the coefficients in the expansion of the potential energy surface (Eq. (3.67)).

For many applications accurate line lists are a prerequisite for detailed modeling of terrestrial, (exo)planet, brown dwarf, or stellar atmospheres. Ab-initio potential energy surfaces – calculated, say, with coupled cluster methods – are used to predict line strengths and frequencies of transitions. These are then compared to high resolution spectroscopic measurements to establish their accuracies and, most importantly, assist in spectral assignments as well as make prediction for higher frequency regimes that are not as amenable to experimental study.

3.3.6 Solid State Vibrational Spectroscopy

Vibrational spectra of molecules frozen into an ice differ in several regards from gas phase spectra. In the solid state, rotations are generally suppressed and hence the rotational–vibrational bands collapse to one absorption band near the band origin. The precise band position will differ from that of the free (gas phase) species due to dispersive, electrostatic, induced, and repulsive interactions with neighboring molecules. For species that can form a

https://doi.org/10.1017/9781316718490.004 Published online by Cambridge University Press

Table 3.6 *Integrated strength of ice bands*

Species	ν [cm^{-1}]	$\Delta\nu$ [cm^{-1}]	A [cm molecule^{-1}]
H_2O	3275	310	2.0 (−16)
H_2O	1670	160	1.0 (−17)
H_2O	750	240	2.8 (−17)
CO	2138	2.5	1.1 (−17)
CO_2	2340	18	7.6 (−17)[a]
CO_2	656	18	1.1 (−17)
CO_2	3708	12	1.4 (−18)
CO_2	3600	19	4.5 (−19)
CH_4	3010	7	1.0 (−17)
CH_4	1300	8	7.3 (−18)
NH_3	3375	45	1.3 (−17)
NH_3	1070	68	1.3 (−17)
CH_3OH	3250	235	1.3 (−16)
CH_3OH	2982	100	2.1 (−17)
CH_3OH	2828	30	5.4 (−18)
CH_3OH	1450	90	1.2 (−17)
CH_3OH	1026	29	1.9 (−17)
OCS	2042	45	1.5 (−16)
OCN^-	2160	25	1.3 (−16)[b]

[a]This band can be strongly affected by small particle scattering effects, which enhance its intrinsic strength (cf. Section 5.2.1). [b]Uncertain. Depends on the assumed efficiency of the production of this species in UV irradiation experiments.

hydrogen-bonded network such as – notably, H_2O but also CH_3OH and NH_3 – these shifts can be up to hundreds wavenumbers. The width of solid state absorption bands likewise depends on the matrix environment. For traces of weakly bonded species in an inert matrix, the width can be as narrow as 0.2 cm^{-1}. An amorphous ice will possess a distribution of binding sites. Variations in the interaction will then broaden the absorption features and width of 2–50 cm^{-1} are expected, denpeding on the mixture. For strong interactions – e.g. species in a H-bonding network – the width can be up to 300 cm^{-1}. For completeness, the far-IR spectral window is home to the phonon modes of solids and these can be used to study interstellar ices as well.

Despite these differences, the general rules for vibrational spectroscopy still hold and IR vibrational spectra provide convenient fingerprints for molecular identification (Figure 3.7, Table 3.5, Section 3.3.3). The absorption properties of some astronomically relevant ices are summarized in Table 3.6. These data refer to pure ices and there is an extensive literature on the effects of matrix variations.

https://doi.org/10.1017/9781316718490.004 Published online by Cambridge University Press

3.4 Electronic Spectroscopy

Here, we will discuss the electronic spectra of simple molecules, with the emphasis on diatomic molecules. The resulting photodissociation cross sections are discussed in Chapter 6.3. The electronic spectra and photophysics of large molecules are discussed in Chapter 8.2.

3.4.1 Energy Levels and Notation

As discussed in Chapter 2, we can classify electrons according to the binding type involved (Figure 3.9): σ-electrons are localized between two atoms and are tightly bound. Transitions involving σ electrons occur therefore at short wavelength (1000–2000 Å). Delocalized π electrons are less strongly bound then σ-electrons and transitions for nonconjugated species are in the far-UV (1500–2500 Å). The energy levels of nonbonding electrons – say associated with lone pair electrons of O or N atoms or nonbonding π electrons – lie typically between those of bonding and antibonding orbitals. According to the Hund's rule, when there are degenerate orbitals, an electron will occupy an empty orbital before it starts to pair up. Typically, excitation of an electron does not affect the spin and, e.g., a singlet ground state (with $S = 0$, see Section 3.4.2) couples with a singlet excited state. For the excited electron, a spin flip can occur, converting, e.g., a singlet state in a triplet state (with $S = 1$). Following Hund's rule, these triplet states are at lower energy than the

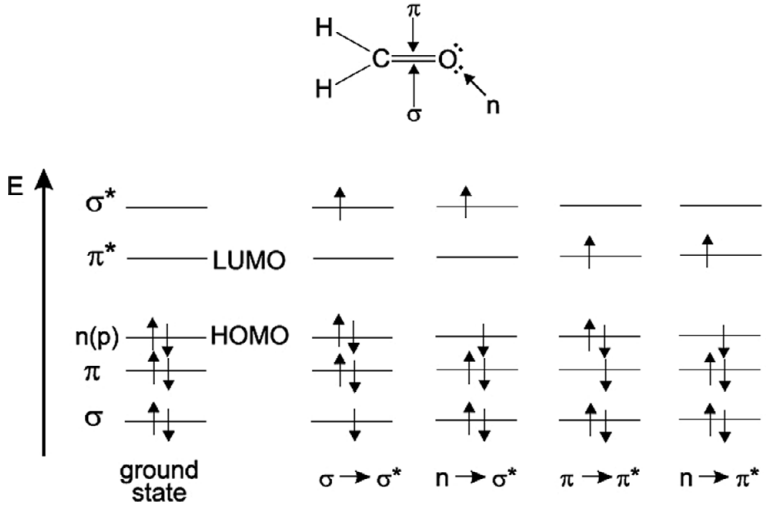

Figure 3.9 Schematic energy diagram for formaldehyde with the various types of electron molecular orbitals and relevant electronic transitions. The left-hand side illustrates the ground state while possible excitations of the different electrons are shown to the right. HOMO stands for highest occupied molecular orbital and LUMO for lowest unoccupied molecular orbital. Figure taken from [16]

https://doi.org/10.1017/9781316718490.004 Published online by Cambridge University Press

corresponding singlet state. Triplet states can connect radiatively with singlet states through spin–orbit coupling,[5] but such transitions have small Einstein A's.

3.4.2 Diatomic Molecules

For atoms, the electronic states are labeled as ${}^{2S+1}L_J$ with L the orbital angular momentum of the electrons (the vector sum of the orbital angular momentum of the individual electrons), S the electron spin angular momentum (the sum of the spins of the individual electrons), and J the total angular momentum (the vector sum of the orbital and spin angular momenta). All of these are in units of $\hbar$. The different values for the total orbital angular momentum, $L = 0, 1, 2, \ldots$, are denoted by roman capitals, S, P, D, ... The electronic states of diatomic molecules are dealt with analoguously but now classified by the projection of their orbital angular momentum on the internuclear axis, $\Lambda = \sum \lambda_i$, their spin multiplicity, S, and the sum of projection of the orbital angular momentum and the spin on the internuclear axis, $|\Omega| = |\Lambda + \Sigma|$: e.g. ${}^{2S+1}\Lambda_\Omega$ with Σ the projection of S on the internuclear axis. The different values for the projected orbital angular momentum, $\Lambda = 0, 1, 2, \ldots$, are labeled as, $\Sigma, \Pi, \Delta, \ldots$. Electronic states of diatomic molecules are also labeled with letters. The ground state is labeled X and excited states with the same multiplicity are labeled $A, B, C, \ldots$ while excited states with different multiplicity are labeled $a, b, c, \ldots$; both are in order of increasing energy. The Pauli exclusion principle requires an overall antisymmetry of the total wavefunction under exchange. The σ states of diatomics are labeled with superscript $+$ or $-$ to indicate symmetry with respect to reflection in a plane containing the internuclear axis. For homonuclear molecules, molecular orbitals are also labeled according to symmetry with respect to inversion through the center of symmetry and the electronic wavefunction is either even (labeled as subscript g for gerade) or odd (labeled as subscript u for ungerade) upon inversion.

3.4.3 Intensity and Franck–Condon Factors

Electronic transitions take place on timescales of femtoseconds ($\Delta t \sim \Delta r/v$ with $\Delta r \sim 10^{-7}$ cm and $v \simeq 10^8$ cm/s). The fastest atomic vibration is associated with CH stretching vibrations and occurs on a timescale of $\simeq 10^{-13}$ s. Hence, essentially, the nuclei are frozen during an electronic transition. This is the basis of the Born–Oppenheimer approximation. The wave function can then be expanded in its electronic (ψ), spin ($\mathcal{S}$), and vibrational (χ) components. The transition probability is then governed by the oscillator strengths,

$$f_e f_{so} f_v \sim \langle \psi | H_e | \psi \rangle \langle \mathcal{S} | H_{so} | \mathcal{S} \rangle \langle \chi | \chi \rangle , \tag{3.69}$$

where the first two terms describe the action of the electronic and spin–orbit coupling Hamiltonians on the wave functions and express the selection rules. The last term is

[5] In a mechanistic view, the magnetic moment associated with the orbital motion of the electron couples with the magnetic moment of the electron spin.

https://doi.org/10.1017/9781316718490.004 Published online by Cambridge University Press

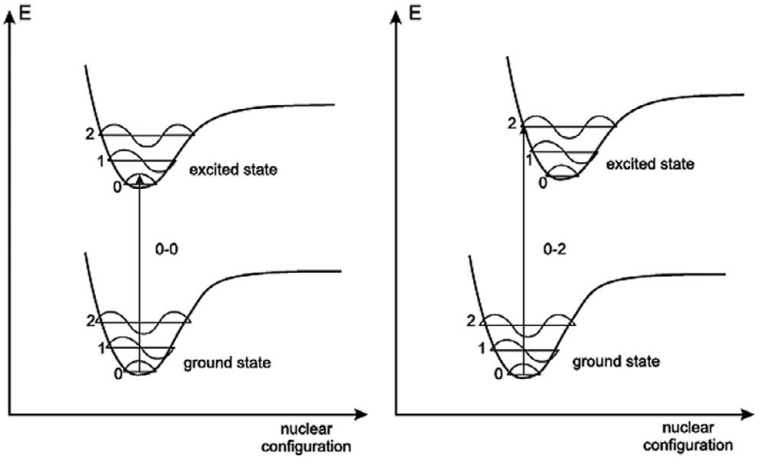

Figure 3.10 Schematic potential energy diagram with wavefunctions, χ, for the various vibrational levels in the ground and excited electronic state. Note that, for excited states, these have highest density near the turning points. Left: The bonding character does not change much between the two electronic states and overlap is largest for the 0–0 transition. Right: The bonding character changes much between the two electronic states and overlap is largest for the 0–2 transition. These two cases will give rise to very different vibrational progressions.

the vibrational overlap and, as there is no electronic action, there are no selection rules for vibrational transitions accompanying electronic transitions. However, the transition strength is governed by the overlap of the vibrational wave functions (Figure 3.10). If the bonding character between the two states is very similar, transitions in the vibrational ground state have the best overlap with the vibrational ground state in the excited electronic state. On the other hand, if the bonding character is very different, the potential energy curves are shifted and the ground vibrational state in the lower electronic state will couple best to an excited vibrational state in the upper electronic state through a vertical transition. Table 3.7 summarizes typical values for longest wavelength electronic transitions of molecular chromophores.

3.5 Specific Examples

Molecular Hydrogen

Following the discussion in Chapter 2, the two 1s orbitals of the H atoms combine into two molecular orbitals. Constructive interference between the two wave functions leads to the highest electron density between the two nuclei and an attractive bonding orbital, which is lower in energy than either atomic orbital. Destructive interference of the wave functions leads to a node (zero electron density) between the two nuclei. This antibonding orbital exceeds the energy of the atomic orbitals. The potential energy diagram of H_2 is shown in Figure 3.11. The configuration of the electronic ground state of H_2 molecule is $\left(1\sigma_g\right)^2$.

https://doi.org/10.1017/9781316718490.004 Published online by Cambridge University Press

Table 3.7 *Long wavelength absorption bands of typical chromophores*[a]

Chromophore	λ [Å]	Absorption strength [cm^2/mol]	Transition
C–C	<1800	1000	$\sigma, \sigma^\star$
C–H	<1800	1000	$\sigma, \sigma^\star$
C=C	1800	10,000	$\pi, \pi^\star$
C=C–C=C	2200	20,000	$\pi, \pi^\star$
Benzene	2600	200	$\pi, \pi^\star$
Naphthalene	3100	200	$\pi, \pi^\star$
Anthracene	380	10,000	$\pi, \pi^\star$
C=O	2800	20	$n, \pi^\star$
N=N	3500	100	$n, \pi^\star$
N=O	6600	200	$n, \pi^\star$
C=C–C=O	3500	20	$n, \pi^\star$
C=C–C=O	2200	20,000	$\pi, \pi^\star$

[a] These correspond to the HOMO → LUMO transition.

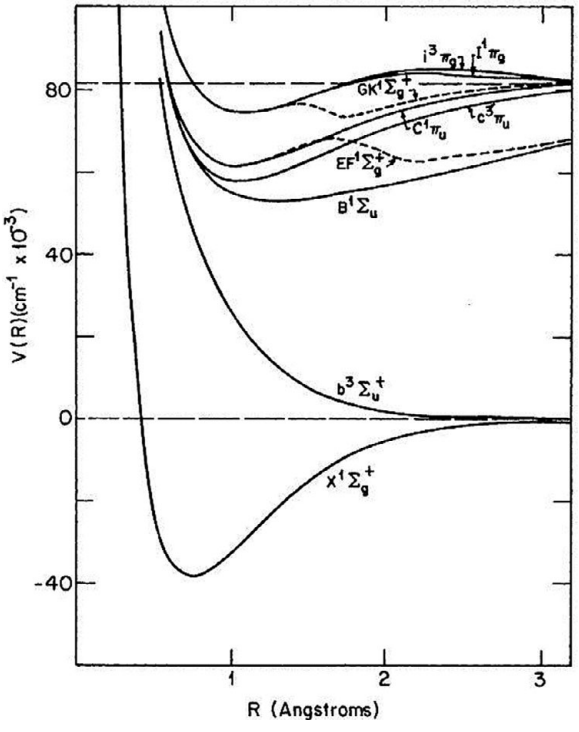

Figure 3.11 Energy level diagram for H_2. The horizontal dashed lines correspond to the energy of the atoms at "infinite" distance (1*s* and 1*s* or 1*s* and 2*s*). Figure taken from [25]

https://doi.org/10.1017/9781316718490.004 Published online by Cambridge University Press

For both electrons, $\lambda = 0$ and hence $\Lambda = 0$, resulting in a Σ state. The electron spin is either $S = 0$ (singlet) or $S = 1$ (triplet). These are antisymmetric and symmetric under exchange. In the ground state, following the Pauli exclusion principle, the electrons will have opposite spins and $S = 0$. As the atomic orbitals are g, the ground state[6] is g. Thus, the ground state is $X\,^1\Sigma_g^+$ followed by the triplet state, $b\,^3\Sigma_u^+$. Higher electronic states couple two H-atoms with $n = 1$ and $n = 2$, for example. The electronic states of H_2^+ are at even higher energies. The ground electronic state of H_2 has 14 bound vibrational states and each of those has an "infinite" number of rotational states. As the nuclei are identical, the combined proton spin is either 0 or 1; e.g. antisymmetric and symmetric under exchange. Molecular hydrogen has para and ortho states (cf. Section 3.2.7). The odd rotational states are ortho ($I = 1$), the even ones are para ($I = 0$), and the statistical weights are 3 and 1 (Section 3.2.7). Selection rules are $\Delta\Lambda = 0, \pm 1$. $\Delta S = 0$, g states couple only to u states and vice versa, and parity is preserved. The change in vibrational quantum number is governed by the Franck–Condon overlap. Within the ground electronic state, there is no restriction on Δv. The pure rotational transitions have to preserve symmetry and occur either fully within the ortho or the para levels. In many ways, ortho and para H_2 behave therefore as separate chemical species that only exchange through chemical reactions (Section 3.2.7).

The $B\,^1\Sigma_g^+$ and $C\,^1\Pi_u^+$ are the next highest singlet states that can couple to the ground electronic state through allowed transitions (the Lyman and Werner band) with typical oscillator strengths of 10^{-2}. Figure 3.12 shows the rich spectrum of H_2 absorption in the Lyman and Werner bands observed toward a star in the Large Magellanic Cloud. Absorptions originate in the various rotational levels of the ground vibrational state in the ground electronic state and connect to ro-vibrational levels of the excited states according to the selection rules.

The vibrational frequency of H_2 in its ground electronic state is at $\nu_e = 4400$ cm^{-1}. As a very light hydride, anharmonicity is relatively important; viz., $\nu_e x_e = 121$ cm^{-1}. As H_2 is a homonuclear molecule, ro-vibrational and pure rotational transitions are dipole forbidden. The vibrational levels in the ground electronic state are still connected through weak quadrupole transitions with $\Delta J = 0 \pm 2$. These transitions are labeled by O(J''), Q(J''), and S(J''), with J'' the lower level rotational quantum number (i.e. 1 − 0 S(1) corresponds to the transition $v' = 1\,J' = 3$ to $v'' = 0\,J'' = 1$). The vibrational levels can be pumped by UV absorption in the Lyman–Werner bands followed by radiative decay as well as by collisions in warm gas. The former is important in diffuse clouds and in photodissociation regions associated with massive stars, planetary nebulae, or galactic nuclei (Section 11.6). The latter can be important in strong shock waves in molecular clouds (Section 11.7). Figure 3.13 shows the near-infrared spectrum observed toward the reflection nebulae, NGC 2023, illuminated by the B0.5 star, HD 37097, revealing strong ro-vibrational H_2 transitions. Because H_2 is such a light hydride, its pure rotational transitions occur at very high frequencies with ground state para ($J = 2$–0) and ortho (3–1) transitions at 28 and 17 μm, respectively.

[6] $g \times g = g$, $u \times u = u$, and $u \times g = g \times u = u$.

https://doi.org/10.1017/9781316718490.004 Published online by Cambridge University Press

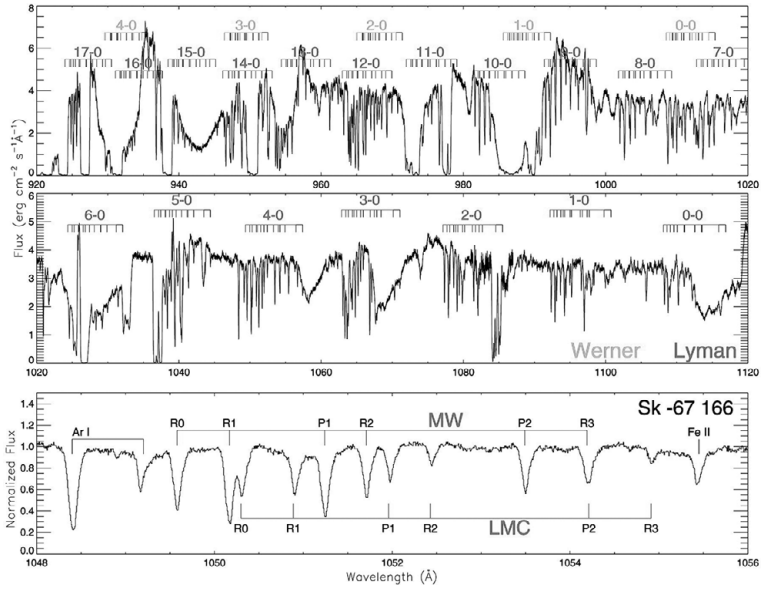

Figure 3.12 The 920–1120 Å absorption spectrum toward the star Sk -67°166 in the Large Magellanic Cloud measured by the Far Ultraviolet Spectroscopic Explorer, FUSE. Various Lyman (black) and Werner (gray) bands are indicated. This rich spectrum shows both LMC and Milky Way absorption components (bottom panel). Figure taken from [31]

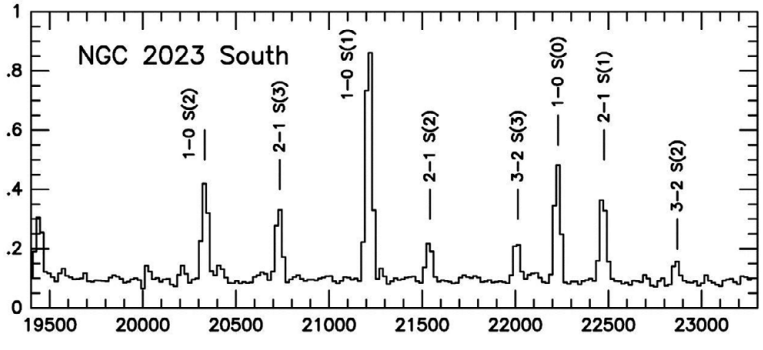

Figure 3.13 The near-IR emission spectrum of the reflection nebula, NGC 2023, revealing H_2 ro-vibrational emission lines associated with $v = 1 - 0$ and $v = 2 - 1$ transitions. Figure taken from [19]

Carbon Monoxide

For CO, we have to mix the atomic orbitals, which we will treat simplistically as one orbital from each center. The orbitals that we mix have to have the same symmetry and need to be close in energy. Thus, $2p_C$ mixes with $2p_O$ and $2s_C$ with $2s_O$ creating bonding and antibonding states (Figure 3.14). Also, s and p_z orbitals mix into σ orbitals (the z-axis is

https://doi.org/10.1017/9781316718490.004 Published online by Cambridge University Press

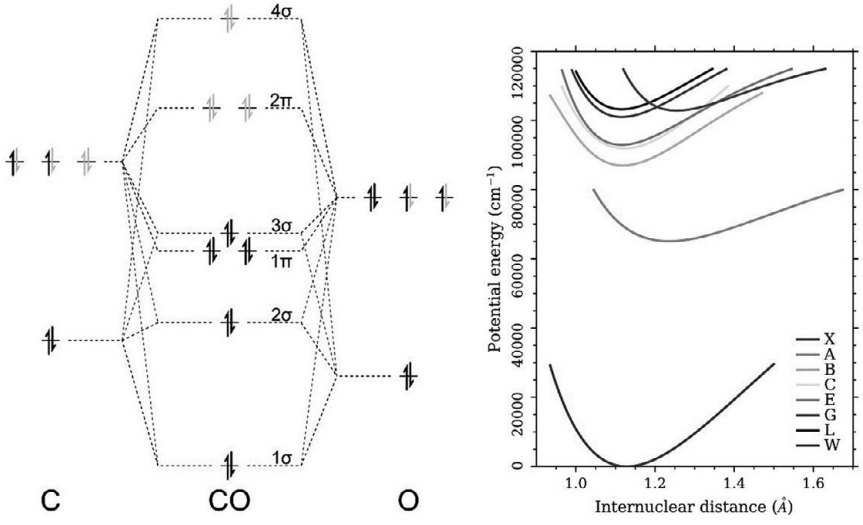

Figure 3.14 Left: Molecular orbitals of CO and their relationship to the atomic orbitals of C and O. As O is more electronegative than C, its orbitals are lower in energy. Right: Energy level diagram for CO. Figure courtesy of [13]

the bond axis) while the p_x and p_y orbitals mix into π orbitals. These states have to be filled and create the electron configuration, $(1\sigma)^2(2\sigma)^2(1\pi_x)^2(1\pi_y)^2(3\sigma)^2$. The wavefunctions of the electrons in the more stable orbits will have the highest electron density near the atom with the highest electron negativity (O). While the higher energy antibonding molecular orbitals will be closer to the less electronegative atoms (C). Thus, reactivity of CO will be concentrated on the C-atom. The total angular momentum and the total spin are both 0 and the ground state is $X\,^1\Sigma^+$. The energy level diagram of CO is shown in Figure 3.14.

Interstellar CO has been studied in the UV through the specific ro-vibrational transitions between the $X\,^1\Sigma^+$ and $A\,^1\Pi$, $B\,^1\Sigma^+$, $C\,^1\Sigma^+$, and $E\,^1\Pi$ states. Photodissociation of CO occurs, amongst others, through absorption into the E states – coupling to C(^3P) and O(^3P) – which predissociate because of an avoided crossing with the W state (Figure 3.14). UV transitions of CO occur in the far ultraviolet and have been measured using spectrographs on, e.g., HST and FUSE in diffuse clouds (Figure 3.15). These and comparable data has been analyzed through a curve of growth-type anaysis (c.f. Section 4.3.2).

The CO $v = 1 - 0$ fundamental vibration occurs at 2170 cm^{-1} (4.61 μm) and has only a modest anharmonicity (13.3 cm^{-1}). The ro-vibrational transitions of CO and its isotopes can be observed through the M-band window in the mid-IR (Figure 3.16) if measured at the right "time" to allow the interstellar transitions to shift out of the atmospheric bands by the Doppler effect due to the Earth's orbital motion. Solid CO is an important component of interstellar ices and its vibrational band is widely detected in absorption in sight lines traversing dense cold molecular clouds (Figure 3.16; see also Section 10.6). Overtone transitions, $\Delta v = 2$ of the CO fundamental are accessible in the K-band.

https://doi.org/10.1017/9781316718490.004 Published online by Cambridge University Press

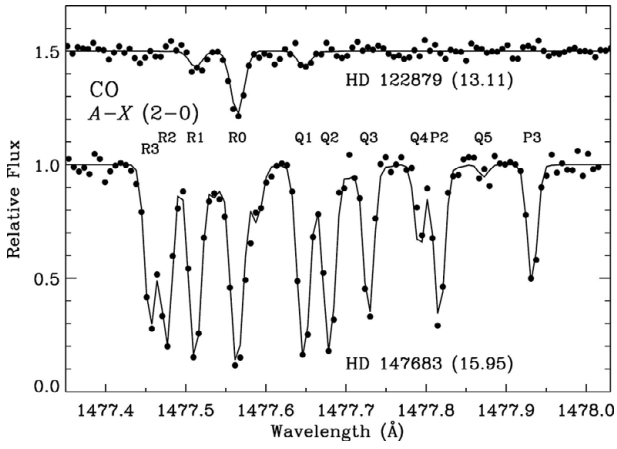

Figure 3.15 UV absorption spectrum measured toward the stars, HD 147683 & 122879, showing absorption lines due to the $A-X$ system. [24]

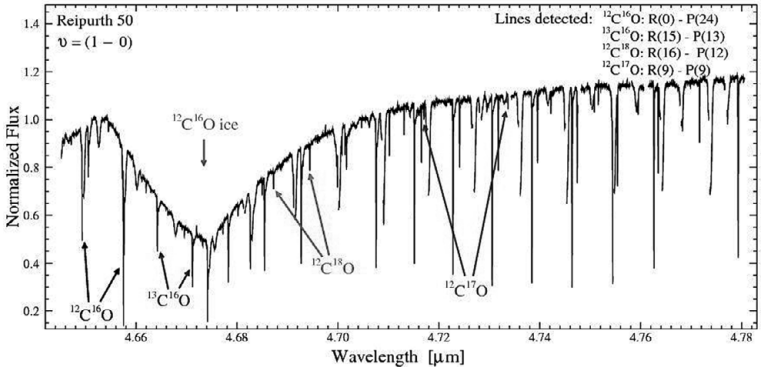

Figure 3.16 Ro-vibrational transitions of CO isotopes in the spectrum of the protostar Reipurth 50. Note also the broad solid CO band [26]

The pure rotational ladder of CO falls in the sub-millimeter and CO transitions are generally observed through the atmospheric windows at high spectral resolution (sub-km/s) and high sensitivity (at the quantum noise level) using heterodyne techniques on single dish telescopes (e.g. IRAM, APEX) or interferometers (e.g. plateau de Bure, ALMA). These instruments typically measure one CO line at a time (albeit that transitions from many other molecules may occur in the same spectral bandpass). Figure 3.18, actually, shows several transitions measured by the SPIRE Fourier Transform Spectrometer on board the Herschel Space Observatory. These observations lack the spectral resolution and have only limited sensitivity but they do obtain a large portion of the CO ladder. Observations of the rotational transitions of CO are widely used to study molecular clouds (Sections 10.1 and 10.2).

https://doi.org/10.1017/9781316718490.004 Published online by Cambridge University Press

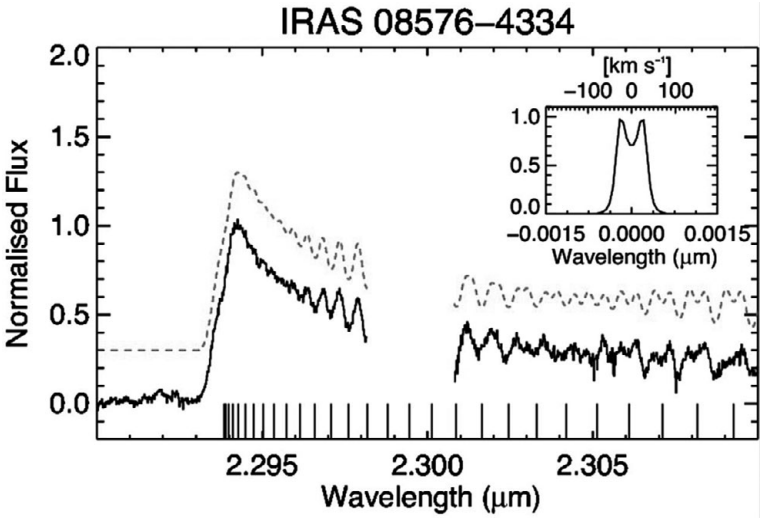

Figure 3.17 The near infrared spectrum of the massive protostar IRAS 08576-4334 reveals the $v = 2 - 0$ transition of CO. Positions of the individual ro-vibrational transitions – shifted to account for the Doppler effect – are indicated below. The dashed trace above the spectrum is a model fit of thee transitions convolved with the adopted line profile shown in the inset. Near the bandhead, the transitions pile up and that allows for an "easy" detection of this feature. Figure courtesy of [14]

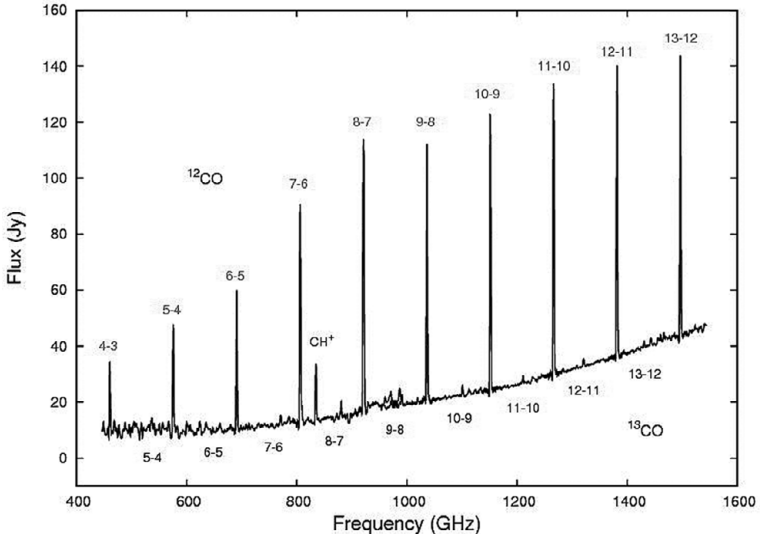

Figure 3.18 The pure rotational spectrum of CO of the planetary nebula, NGC 7027, measured by the SPIRE instrument on the Herschel Space Observatory. ^{12}CO lines are labeled at the top. ^{13}CO lines are labeled at the bottom. Figure courtesy of [32]

https://doi.org/10.1017/9781316718490.004 Published online by Cambridge University Press

Polyatomic Molecules

The electron-level diagram for polyatomic molecules quickly becomes very complex. As an example, consider H_2CO (Figure 3.9). Following the discussion in Chapter 2 and ignoring the $1s$ electrons, the electron configuration of C is $(2s)^2(p_x)(p_y)$, where the p_x and p_y orbitals each have one electron with parallel spin and the $2p_z$ orbital is empty. One of the $2s$ electrons is promoted to the $2p_z$ orbital. The $2s$ orbitals hybridize with the two $2p$ orbitals to form three sp^2 orbitals (each with one electron). Overlap between two sp^2 hybridized orbitals of C with the $1s$ orbitals of the two H's gives rise to two σ bonds. The third sp^2 orbital of C overlaps with the oxygen sp^2 orbital, resulting in a σ_{CO} bond while overlap of the p_z orbitals on the C and O atoms gives rise to a π_{CO} bond. In addition, oxygen has two lone pairs of electrons, which are in nonbonding orbitals, n_O. Because of the higher electronegativity of O versus C, the energies of the molecular orbitals increase as, $1s_O < 1s_C < 2s_O < \sigma_{CH} < \sigma_{CO} < \pi_{CO} < n_O$ where the first three are essentially pure atomic orbitals, and the others are the σ, π, and nonbonding orbitals. The ground state configuration is then,

$$(1s_O)^2(1s_C)^2(2s_O)^2(\sigma_{CH})^2(\sigma'_{CH})^2(\sigma_{CO})^2(\pi_{CO})^2(n_O)^2(\pi^\star_{CO})^0 \tag{3.70}$$

In low-lying states, an n electron or a π electron can be promoted to a $\pi^\star$ orbital (Figure 3.9) and the electron spins can be parallel (triplet state) or antiparallel (singlet states). The ground state is $X\,^1A_1$ and excited states are $A\,^1A_2(n,\pi^\star)$ and $B\,^1A_1(\pi,\pi^\star)$. These states are labeled as S_0 ($^1A_1$) and S_1 ($^1A_2$) and T_1 ($^3A_2$).[7] Groundstate formaldehyde shows strong $\pi \rightarrow \pi^\star$ transitions around 1870 Å, while the $n \rightarrow \pi^\star$ transitions are much weaker (as there is little overlap between these essentially orthogonal orbitals) and occur around 2850 Å.

In the ISM, formaldehyde is observed through its pure rotational levels. The rotational level diagram of this near-prolate molecule is shown in Figure 3.3 and discussed in Section 3.2.4. The rotational transitions of formaldehyde provide a good tool for studies of physical conditions in dense molecular cloud cores (cf. Section 4.2.3) and are often used for this purpose, particularly for star-forming cores (Section 10.1). Gaseous formaldehyde has also been observed through its ν_1 and ν_5 symmetric and asymmetric CH_2 stretching vibrations around 3.6 μm in absorption in the spectrum of protostars and in emission in the spectrum of comets.

3.6 Further Reading and Resources

There are many textbooks that deal with atomic and molecular structure and transitions. For astrophysics, references [3, 22, 27, 30] provide comprehensive overviews. Conventions for line strength are detailed in [33] and line strengths of molecules are conveniently tabulated in appendix V of [30]. [1] provides a tutorial on the strength of (hyper)fine-structure lines. [18] treats in detail the conversion of observed line intensities into molecular column densities.

[7] For large molecules, nomenclature changes and the ground state, if singlet as for formaldehyde, is labeled S_0 while excited singlet states are labeled, $S_1 \ldots S_n$ and triplet states are labeled as $T_1, \ldots T_n$.

https://doi.org/10.1017/9781316718490.004 Published online by Cambridge University Press

The PGOPHER program simulates rotational, vibrational, and electronic spectra and is accessible at http://pgopher.chm.bris.ac.uk/index.html. HITRAN (high-resolution transmission) database (https://hitran.org) provides a compilation of spectroscopic parameters that can be used to simulate infrared spectra. While HITRAN is developed for atmospheric research, the database is also very useful for astronomical purposes. Reference [23] provides more details on developing line lists. The ExoMol database, http://exomol.com/, provides accurate, evaluated line lists for relevant species. The field has been reviewed by [4].

Information on spectroscopy and excitation of atoms and molecules can be found at the website of the NIST (www.nist.gov/srd/atomic.htm) & https://physics.nist.gov/cgi-bin/micro/table5/start.pl. Rotational spectra of molecules can also be accessed through the website maintained by JPL (http://spec.jpl.nasa.gov/) and the Cologne Database for Molecular Spectroscopy (www.ph1.uni-koeln.de/vorhersagen/).

References [7, 12] provide early studies on the characteristics of IR spectra of astronomically relevant ice species. Studies on CO and CO_2 are particularly relevant [2, 9, 29]. Far-infrared properties of relevant ices are rarer. An early review is [21] and a recent study using THz timedomain spectroscopy is provided by [11]. Databases of laboratory spectra of interstellar ice analogs are available at: http://icedb.strw.leidenuniv.nl/, https://science.gsfc.nasa.gov/691/cosmicice/constants.html, and www.astrochem.org/databases.php.

3.7 Exercises

3.1 Transition frequencies

(a) Consider an electron in orbit around the nucleus. For a typical energy of 5 eV, what is the photon frequency required to move the electron out by 1 Å?

(b) In a similar fashion, atoms in a molecule can be considered connected by springs. Show that vibrational and electronic frequencies are then related roughly by $\sqrt{m_e/M}$.

(c) Show that, for rotations, the relationship is m_e/M.

3.2 Explain the difference between the rotational frequencies of CO and CS.

3.3 The $J = 2 \rightarrow 1$ rotational transition of $^{12}C^{16}O$ occurs at 230.538MHz. What is the bond length? What would you predict the $J = 2 \rightarrow 1$ transition of $^{13}C^{16}O$ to be?

3.4 Centrifugal distortion:

(a) A real molecule is not rigid and the contrifugal force will lead to an increased bond length when the molecule rotates faster. Consider a harmonic vibration where the restoring force is given by $-\kappa\,(R_e - R)$. The centrifugal force is given by $M\omega^2 R$. Balancing these two forces, use the quantized form of the angular momentum, to show that

$$R = R_e + \frac{J\,(J+1)\,\hbar^2}{M\kappa R^3}, \tag{3.71}$$

and thus that the nuclear separation increases with increasing rotation.

https://doi.org/10.1017/9781316718490.004 Published online by Cambridge University Press

(b) Use Hooke's law to show that $R = R_e\,(1+\delta)$, where the small correction factor δ is given by,

$$\delta = \frac{J\,(J+1)\,\hbar^2}{M\kappa R_e^4}. \tag{3.72}$$

(c) The potential energy is then larger by $\kappa\,(R-R_e)^2\,/2$. Show that this results in,

$$E_{rot} = \frac{J\,(J+1)\,\hbar^2}{2MR_e^2} - \frac{J^2\,(J+1)^2\,\hbar^4}{2M^2\kappa R_e^6}. \tag{3.73}$$

(d) Show that this implies that for harmonic vibrations, D_e is given by $4B_e^3/\nu_e^2$.

(e) In this derivation, we have made the assumption that $\delta \ll 1$. Show that this is justified for CO.

3.5 Formaldehyde is a nearly prolate molecule with $A = 281970.37$, $B = 38835.42558$, and $C = 34005.73031$ all in MHz. Calculate the energy level diagram for the prolate molecule with $A' = A$ and $B' = C' = (B+C)\,/2$ and compare with the energy levels of H_2CO.

3.6 Rotational partition function.

(a) Linear rigid rotor:

(i) Derive the expression for the partition function of a linear rigid rotor (Eq. (3.32)) by making the transition from a summation to an integral, the substitution, $x = E\,(J)\,/kT$, and assuming that $T \gg hB/k$.

(ii) Adopting $T = 10\text{K}$, $B = 2\,\text{cm}^{-1}$ compare this approximate expression with the actual summed partition function. For what temperature is the approximation better than 10%?

(b) Derive the expression for the partition function of a rigid symmetric top following these steps:

(i) Write the partition function as a summation over the J and K states.

(ii) The energy is a function of J and K where J runs from 0 to ∞ and K from $-J, \ldots, 0 \ldots, J$ but this can also be seen as $K = 0, \ldots, \infty$ and $J = K, \ldots \infty$. Rewrite the equation for the partition function to reflect this.

(iii) Make the transition to integrals.

(iv) Do the integral over J first (see above).

(v) Realize that $K\,(K+1) \simeq K^2$. Do the integral over K.

(c) Consider the following intuitive derivation of the expression for the partition function of a rigid asymmetric top:

(i) Consider the partition function as a sum over all angular momentum states, L_a, L_b, and L_c, which we will assume, each, to run from $-\infty$ to ∞. Convert the summations to integrations, which yields for each axis, $\sqrt{2\pi I_i kT}$.

https://doi.org/10.1017/9781316718490.004 Published online by Cambridge University Press

(ii) This has to be multiplied by $8\pi^2$. For a chosen axis, the angular integration yields a factor 2π. The integration over the orientation of this axis gives an additional factor of 4π.
(iii) Make the transition from classical to quantum mechanics.

3.7 Symmetry factor:

(a) What is the symmetry factor for H_2?
(b) What is the symmetry factor for H_2O?
(c) What is the symmetry factor for NH_3?
(d) What is the symmetry factor for CH_4?
(e) What is the symmetry factor for C_6H_6?

3.8 Consider a harmonic oscillator. Combine Newton's law with Hooke's restoring force and solve for a sinusoidal motion to derive the normal mode frequency.

3.9 The fundamental frequency of HCl is at 2886 cm^{-1}. What is its force constant? For CO, the fundamental frequency occurs at 2170 cm^{-1}. What two factors play a role in this difference with HCl?

3.10 The fundamental asymmetric stretching vibration of carbon monoxide occurs at 2143 cm^{-1}. The first overtone is at 4260 cm^{-1}.

(a) What are the harmonic vibrational frequency and the anharmonic constant?
(b) Predict the frequency of the second overtone.
(c) The second overtone occurs at 6350 cm^{-1}. What could be the origin of the discrepancy?
(d) Estimate the bond energy of this molecule.

3.11 The fundamental asymmetric CH stretching vibration of methane occurs at 3019 cm^{-1}. The first overtone is at 6006 cm^{-1}.

(a) What are the harmonic vibrational frequency and the anharmonic constant?
(b) Predict the frequency of the second overtone.
(c) Estimate the CH bond energy.

3.12 The vibrational partition function:

(a) Water has three vibrational modes at 3657, 1595, and 3758 cm^{-1}. Calculate the vibrational partition function at 300 K and at 1500 K.
(b) Carbon dioxide has vibrational modes at 1388, 667, and 2349 cm^{-1} where the 667 cm^{-1} mode is doubly degenerate. Calculate the vibrational partition function at 300 K and at 1500 K and compare to those of water.
(c) Consider now a 72-atom molecule (say, circumcoronene ($C_{54}H_{18}$)). Assume that each of the vibrational modes in this species has the (geometric) average partition function of a mode in the water molecule. Calculate the vibrational partition function of this molecule at 300 and 1500 K.

https://doi.org/10.1017/9781316718490.004 Published online by Cambridge University Press

(d) Evaluate the partition function of this large molecule assuming the average CO_2 vibrational partition function.
(e) Compare these partition functions – marvel – and then draw reasoned conclusions on the importance of the temperature and the vibrational frequency spectrum.

Bibliography

[1] Axner, O., Gustafsson, J., Omenetto, N., Winefordner, J. D., 2004, *Spectro Chim Acta B*, 59, 1
[2] Baratta, G. A., Palumbo, M. E., 2017, *A & A*, 608, A81
[3] Bernath, P., 2005, *Spectra of Atoms and Molecules* (Oxford: Oxford University Press)
[4] Bernath, P., 2020, *J Quant Spectr Rad Trans*, 240, 1
[5] Cooksy, A. L., Blake, G. A., Saykally, R. J., 1986, *ApJ*, 305, L89
[6] Darling, J., Zeiger, B., 2012, *ApJL*, 749, L33
[7] d'Hendecourt, L. B., Allamandola, L. J., 1986, *A & A Suppl*, 64, 453
[8] DiSanti, M. A., Bonev, B. P., Magee-Sauer, K., et al., *ApJ*, 650, 470
[9] Ehrenfreund, P., Boogert, A. C. A., Gerakines, P. A., et al., 1996, *A & A*, 315, L341
[10] Gray, M., *Maser Sources in Astrophysics*, (Cambridge: Cambridge University Press)
[11] Giuliano, B. M., Gavdush, A. A., Müller, B., et al., 2019, *A & A*, 629, A112
[12] Hagen, W., Tielens, A. G. G. M., Greenberg, J. M., 1983, *A & A Suppl*, 51, 389
[13] Heays, A., private communication
[14] Ilee, J. D., et al., 2014, *MNRAS*, 429, 2960
[15] Klein, H., Lewen, F., Schieder, R., Stutzki, J., Winnewisser, G. 1998, *ApJ*, 494, L125
[16] Liao, Y.-Y., 2013, PhD Thesis, Ecole Normale Superieure de Cachan
[17] Mangum, J. G., Wootten, A., 1993, *ApJS*, 89, 123
[18] Mangum, J. G., Shirley, Y. L. 2015, *Publ Astron Soc Pacific*, 127, 266
[19] Martini, P., Sellgren, K., DePoy, D. L., 1999, *ApJ*, 526, 772
[20] Mina-Camilde, N., Manzanares, C., 1996, *J Chem Educ*, 73, 805
[21] Moore, M. H., Hudson, R. L., 1994, *A & A Suppl*, 103, 45
[22] Pradhan, A. K., Nahar, S. N., 2011, *Atomic Astrophysics and Spectroscopy* (Cambridge: Cambridge University Press)
[23] Schwenke, D. J., *J Phys Chem*, 1996, 100, 2867
[24] Sheffer, Y., Rogers. M., Federman, S. R., et al., 2008. *ApJ*, 687. 1075
[25] Shull, J. M., Beckwith, S., 1982, *Annu Rev Astron Astrophys*, 20, 163
[26] Smith, R., Pontoppidan, K. M., Young, E. D., et al., 2009, *ApJ*, 701, 163
[27] J. Tennyson, *Astronomal Spectroscopy* (World Scientific)
[28] Tennyson, J., Yurchenko, S. N., Al-Refaie, A. F., et al., 2016, *J Mol Spec*, 127, 73
[29] Tielens, A. G. G. M., Tokunaga, A. T., Geballe, T. R., Baas, F., 1991, *ApJ*, 381, 181
[30] Townes, C. H., Schalow, A. L., 1955, *Microwave Spectroscopy* (New York: McGraw-Hill)
[31] Tumlinson, J., Shull, J. M., Rachford, B. L., et al., 2002, *ApJ*, 566, 857
[32] Wesson, R., Cernicharro, J., Barlow, M. J., et al., 2010, *A & A*, 518. L144
[33] Whiting, E. E., Schadee, A., Tatum, J. B., Hougen, J. T., Nicholls, R. W., 1980, *J Mol Spectr*, 80, 249
[34] Yamamoto, S., Saito, S. 1991, *ApJ*, 370, L103